Bio-Inspired Urea Dosing and NOx Conversion
using a Biomimetic Effervescent Injector

Larsson, Peter

2019

Document Version:
Publisher's PDF, also known as Version of record

Link to publication

Citation for published version (APA):
Larsson, P. (2019). *Bio-Inspired Urea Dosing and NOx Conversion: using a Biomimetic Effervescent Injector*. Department of Energy Sciences, Lund University.

Total number of authors:
1

LUND UNIVERSITY

PO Box 117
221 00 Lund
+46 46-222 00 00

Bio-Inspired Urea Dosing and NOx Conversion

Bio-Inspired Urea Dosing and NOx Conversion
using a Biomimetic Effervescent Injector

by Peter Larsson

Thesis for the degree of Doctor of Philosophy
Thesis advisors: Prof. Per Tunestål
Faculty opponent: Dr. Yiqun Huang

To be presented, with the permission of the Faculty of Engineering of Lund University, for public criticism in the M:B lecture hall at the M-Building, LTH on Thursday, the 28th of March 2019 at 10:00.

DOKUMENTDATABLAD enl SIS 61 41 21

Organization
LUND UNIVERSITY

Department of Energy Sciences
Box 188
SE–221 00 LUND
Sweden

Document name
DOCTORAL DISSERTATION

Date of disputation
2019-03-28

Sponsoring organization

Author(s)
Peter Larsson

Title and subtitle
Bio-Inspired Urea Dosing and NOx Conversion: using a Biomimetic Effervescent Injector

Abstract
Transport of people and freight on-road have a big impact on the total energy use in the world. The majority of these transports is propelled with diesel engines and the reason is simply that the diesel engine is better than the gasoline engine due to lower fuel consumption. But the cost of this is the increase in dangerous nitrogen oxides (NOx). Around 10 000 people dies every year due to emissions emitted by diesel engines and the majority is caused by NOx emissions. If new technology could be applied and improve today's exhaust after-treatment systems, more than 174 000 lives can be saved by year 2040. This thesis focuses on a technology developed by Swedish Biomimetics 3000 in cooperation with Lund University. The technology is novel in it's way to introduce small pre-heated droplets into the stream of exhaust gases and this method is inspired by nature. These droplets evaporate a lot faster compared to the standard system's today. Tests have shown that this new technology is able to reduce the NOx emissions and at the same time reduce the unwanted slip of ammonia through the catalyst. To further reduce the total NOx emitted during the full engine up-time the catalyst needs to be warmed-up faster and enable high NOx-conversion earlier. The pre-heated droplet's don't lower the exhaust temperature as much as today's standard systems and does not require as high light-off temperature.
Results from this investigation shows that high conversion rates are possible already at temperatures below 200°C. The reason is mainly due to the 87% reduction in droplet sizes. An effect of this is also that the total conversion rate can be increased drastically.
This technology can be used on both heavy-duty and light-duty vehicles. The enhanced evaporative process has also show that the flow restricted mixer functions can be reduced which then lowers the back-pressures and the engine can be operated more efficiently. This leads to a reduction of CO_2 as an GHG-emissions due to the reduction in fuel consumption.

Key words
Bio-Inspired, Biomimetics, Bombardier Beetle, AdBlue, DEF, AUS-32, SCR, Exhaust After-treatment, Dosing, Nitrogen Oxides

Classification system and/or index terms (if any)

Supplementary bibliographical information

Language
English

ISSN and key title
<0282-1990>

ISBN
978-91-7895-024-9 (print)
978-91-7895-025-6 (pdf)

Recipient's notes

Number of pages
115

Price

Security classification

I, the undersigned, being the copyright owner of the abstract of the above-mentioned dissertation, hereby grant to all reference sources the permission to publish and disseminate the abstract of the above-mentioned dissertation.

Signature ____________________ Date 2019-03-04

Bio-Inspired Urea Dosing and NOx Conversion
using a Biomimetic Effervescent Injector

by Peter Larsson

LUND UNIVERSITY

A doctoral thesis at a university in Sweden takes either the form of a single, cohesive research study (monograph) or a summary of research papers (compilation thesis), which the doctoral student has written alone or together with one or several other author(s).

In the latter case the thesis consists of two parts. An introductory text puts the research work into context and summarizes the main points of the papers. Then, the research publications themselves are reproduced, together with a description of the individual contributions of the authors. The research papers may either have been already published or are manuscripts at various stages (in press, submitted, or in draft).

Funding information: The thesis work was financially supported by the Swedish Energy Agency, grant number 36013-1, 43354-1 and Swedish Biomimetics 3000® AB

Faculty of Engineering, Department of Energy Sciences

ISBN: 978-91-7895-024-9 (print)
ISBN: 978-91-7895-025-6 (pdf)
ISSN: <0282-1990>

Printed in Sweden by Tryckeriet i E-Huset, Lund University, Lund 2019

To my late father
Sven-Åke Larsson †2018

Contents

List of publications

This thesis is based on the following publications, referred to by their Roman numerals:

I **A Droplet Size Investigation and Comparison Using a Novel Biomimetic Flash-Boiling Injector for AdBlue Injections**

P. Larsson, W.Lennard, O.Andersson, P. Tunestål
SAE Technical Paper 2016-01-2211, 2016

II **NOx-Conversion and Activation Temperature of a SCR-Catalyst Whilst Using a Novel Biomimetic Flash-Boiling AdBlue Injector on a LD Engine**

P. Larsson, W.Lennard, J.Dahlström, Ö.Andersson, P. Tunestål
SAE Technical Paper 2016-01-2212, 2016

III **SCR-Catalyst Utilisation and Mixing Comparison using A Novel Biomimetic Flash-Boiling Injector**

P. Larsson, P.Ravenhill, L-U.Larsson, P. Tunestål
Conf. Proc. ASME ICEF2018-9763, 2018, San Diego, USA

IV **NOx-Conversion Comparison of a SCR-Catalyst Using a Novel Biomimetic Effervescent Injector on a Heavy-Duty Engine**

P. Larsson, P. Ravenhill, P.Tunestål
SAE Technical Paper 2019-01-0047, 2019

Acknowledgements

First I would like to direct a special thank to my supervisor Per Tunestål. Without your knowledge and support this project would definitely not be this successful. Also thank you very much for all the other discussions and soccer game invites during the years.

I would also like to thank Lars-Uno Larsson my employer at Swedish Biomimetics 3000 AB for keeping me around all this years and by extensive work was able to co-finance the project from the start to the end. Thank you very much! Also at SB3000 I want thank my closest colleagues and manager's Will Lennard and Paul Ravenhill for your great work in program management, technical expertise and design work. I do appreciate your time spent discussing the program as well as other not work related things.

Special thanks goes also to Öivind Andersson, Martin Tunér and Sebastian Verhelst for all the good mood and great discussion during office hours and fika breaks.

Definitely this project wouldn't see the end without the participation from the "men in blacks", the technicians Patrik, Anders, Tomas, Tommy and Martin for...well everything in the lab to make the engines work. Also the lab chief Marcus for letting me "harass" them with all my special needs in making parts and so forth.

My time in Lund had not be the same without my brother in arms, Ted Lind. Thank you a lot for all the good time we had and yet to come.

I would also like to thank my other colleagues in Lund, Nhut, Mike, Kenan, Pablo, Erik, Sam and Nico for all the good talks during office hours, lunches and fika breaks.

Coming towards the end of this acknowledgements I would like to thank my family and friends outside of work for all the moral support and that you have always believed in what I am doing. Thank you very much!

Last but not least, Tina my best friend and life partner. Thank you for everything that you do and that you bare with me through every ups and downs that comes with doing a PhD and writing a thesis. Also our lovely children Elsa and Herman for keeping us busy and happy as well as reminding us the importance in life. Thank you from the bottom of my hearth!

Popular summary in English

Transport of people and freight on-road have a big impact on the total energy use in the world. The majority of these transports is propelled with diesel engines and the reason is simply that the diesel engine is better than the gasoline engine due to lower fuel consumption. But the cost of this is the increase in dangerous nitrogen oxides (NOx). Around 10 000 people dies every year due to emissions emitted by diesel engines and the majority is caused by NOx emissions. If new technology could be applied and improve today's exhaust after-treatment systems, more than 174 000 lives can be saved by year 2040.

The most common way to treat NOx emissions to more harmless nitrogen and water is with a technology called Selective Catalytic Reduction (SCR). This technology uses an aqueous urea solution, more commonly known as AdBlue in Europe or DEF in USA. This solution is injected into the stream of exhaust gases prior the catalyst. The water content in the solution needs to be evaporated between the point of injection and the front side of the catalyst in order to treat the NOx emissions most efficiently.

The content of this thesis focuses on a technology developed by Swedish Biomimetics 3000 in cooperation with Lund University. The technology is novel in its way to introduce small pre-heated droplets into the stream of exhaust gases and this method is inspired by nature. Theses droplets evaporate a lot faster compared to the standard system's today. Tests have shown that this new technology is able to reduce the NOx emissions and at the same time reduce the unwanted slip of ammonia through the catalyst. To further reduce the total NOx emitted during the full engine up-time the catalyst needs to be warmed-up faster and enable high NOx-conversion earlier. The pre-heated droplet's don't lower the exhaust temperature as much as today's standard systems and does not require as high light-off temperature.

Results from this investigation shows that high conversion rates are possible already at temperatures below 200°C. The reason is mainly due to the 87% reduction in droplet sizes. An effect of this is also that the total conversion rate can be increased drastically.

This technology can be used on both heavy-duty and light-duty vehicles. The enhanced evaporative process has also show that the flow restricted mixer functions can be reduced which then lowers the back-pressures and the engine can be operated more efficiently. This leads to an reduction of CO_2 as a GHG-emissions due to the reduction in fuel consumption.

Populärvetenskaplig sammanfattning på svenska

Transport av människor och gods på väg står för en stor del av världens energianvänding och dessa transporter sker nästan uteslutande med dieselmotorer. Anledningen är att dieselmotorn är bättre än bensinmotorn i dessa avseenden pga sin jämförelsevis låga bränsleförbruking. Men den stora nackdelen med denna motorn är dess utsläpp av kvävedioxider. Ungefär 10 000 människor dör årligen pga utsläpp från dieselmotorerna och den allra största anledningen är just kvävedioxider. Med hjälp av förbättrad avgasefterbehandling kan upp till 174 000 människoliv sparas fram till år 2040.

Det absolut vanligaste sättet att omvandla farliga kvävedioxider till kvävgas och vatten är med hjälp av en teknik vid namn SCR. Denna teknik använder en urealösning, mest känd som AdBlue i Europa eller DEF i USA, som tillsätts innan katalysatorn. På vägen mellan doseringspunkten och början på katalysatorn måste vattnet i lösningen kokas bort för att urean ska kunna omvandlas till ammoniak som då kan reagera med kvävedioxiderna.

Denna avhandling fokuserar på en teknik som Swedish Biomimetic 3000 AB tillsammans med Lunds Universitet har utvecklat. Denna teknik bygger på en ny typ av insprutningsteknologi för att tillsätta urealösning på ett effektivare sätt till avgaserna. Små droppar som dessutom är förvärmda doseras in i avgasflödet och förångas mycket snabbare än dagens teknologi. Tester har visat att denna tekniken kan minska utsläppet av de farliga kväveoxiderna och samtidigt även minska oönskade genomströmningen av ammoniak efter katalysatorn. För att ytterligare kunna minska de totala utsläppen så måste katalysatorn värmas upp snabbare så omvandling kan ske tidigare under fordonets drift, med andra ord under kall-start. Dessa förvärmda dropparna minskar inte avgastemperaturen lika mycket som dagens teknik och kräver inte heller lika hög start temperatur för att kunna förångas.

Tester i denna avhandling har visat på en hög omvandlingsgrad under 200°C. Förklaring till detta är just den 87%-iga minskningen av droppstorleken jämfört med dagens teknologier. Detta har även medfört att den totala omvandligen kan minska drastiskt. Denna tekniken är applicerbar på både befintlig SCR-teknik för personbilar och lastbilar. Den förbättrade förångingsprocessen har även visat att man kan ta bort blandaren innan katalysatorn vilket då minskar mottrycket och motorn kan arbeta effektivare. Detta bidrar då till en minskad bränsleförbrukning vilket ger minskade växthusgasutsläpp i form av koldioxid.

Abbreviations and Symbols

ANR	Ammonia to NOx Ratio
BDC	Bottom dead center
CAD	Crank angle degree
CI	Compression ignition
CO	Carbon monoxide
$\mathbf{CO_2}$	Carbon dioxide
DI	Direct injection
EGR	Exhaust gas recirculation
EOI	End of injection
ESC	European stationary cycle
ETC	European transient cycle
GHG	Greenhouse gases
$\mathbf{H_2O}$	Water
HC	Hydrocarbon
HD	Heavy duty
ICE	Internal combustion engine
IMEP	Indicated mean effective pressure
LD	Light duty
$\mathbf{N_2}$	Nitrogen
$\mathbf{NH_3}$	Ammonia
$\mathbf{NO}_x$	Nitrogen oxides
$\mathbf{O_2}$	Oxygen
PFI	Port fuel injection
PM	Particulate matter
PN	Particulate number
SCR	Selective catalytic reduction
SI	Spark ignition
SOC	Start of combustion
SOI	Start of injection
TDC	Top dead center
TWC	Three-way catalyst
UHC	Unburnt hydrocarbons
WHSC	World harmonized stationary cycle
WHTC	World harmonized transient cycle
λ	Lambda
θ	Mean value
ϕ	Equivalence ratio
σ	Standard deviation
η_T	Thermal efficiency
r_c	Compression ratio
γ	Specific heat ratio

Chapter 1

Introduction

1.1 Introduction

Freight and other kinds of transportation by road vehicles keep increasing over the years and it is projected that freight mileage will be doubled by 2050 if compared to todays numbers [12]. A significant part of this increase comes from growing Non-OECD countries [20]. The transport sector has seen a significant decrease of harmful emissions such as NOx and soot, with the push from the legislation [10]. But even though the harmful emission is close to zero within most of the OECD countries the rest of the world is behind in the emission legislation. One of the largest problems is the local NOx emissions. Today the pollution from the emissions causes over 10 000 pre-mature deaths annually and even with today's levels this number is expected to increase with the growth of the transport sector [2].

In order to reduce this problem more research is needed in the field of exhaust after-treatment to reduce the NOx even further, especially for the real-driving emissions RDE [24]. If new technology is able to push the development even further beyond EURO 6/VI it is predicted that up to 174 000 lives can be saved by 2040 [2].

Today the most used exhaust after-treatment technology is Selective Catalytic Reduction (SCR) [1]. This system relies greatly on the AUS-32, more commonly known as AdBlue or DEF, evaporation prior the catalyst and fast catalyst heat-up during the cold-start phase of the engine, in order to enable high NOx reduction early and during a longer period of time.

1.2 Objectives

The aim for this thesis is to expand the knowledge on SCR-technology and the potential benefits of adding a completely new AUS-32 dosing method to the already existing technology. This new dosing method has been developed within the scope of this thesis for AUS-32 dosing and the technology is inspired by nature and specifically from the Bombardier beetle.

Previous research has shown that the spray mechanism generated by the beetle can be implemented in a mechanical spray unit [3]. This spray technology has also shown that by using an additional heat source to a liquid contained within a constant volume chamber a fine spray of gasoline can be port fuel injected into an inlet manifold of an SI engine [4]. The question is if this technology also can have an impact on NOx reduction by dosing a pre-heated spray into the stream of exhaust gases prior the SCR-catalyst.

1.3 Thesis Contribution

The results within this thesis contributed with knowledge on how a novel injector technology can reduce the harmful NOx emissions using an existing SCR-technology. This thesis introduces the novel technology and by experimental spray investigation using a laser diffraction technique in a spray rig explains the spray performance of the system. These results are then transferred over to experimental studies on a light-duty diesel engine equipped with a standard SCR-catalyst focusing on NOx-reduction, activation temperature and mixing performance. The last part of this thesis contribution is to explain the behaviour on a heavy-duty engine focusing on NOx-reduction and ammonia slip measurement using a diode laser gas analyser based on specific light absorption of the target gas composition.

1.4 Outline

Chapter 2

This chapter describes the diesel engine concept and why this engine is used for the majority of the freight transporting vehicles. It explains the history and part of the development up to today's modern diesel engines. In order to achieve a great impact on reducing the NOx emission it is also important how these harmful emissions is formed.

Chapter 3

NOx-reduction of diesel exhaust gases can be conducted with various technologies such as the targeted selective catalytic reduction. But there are also other concepts such as selective non-catalytic reduction, lean NOx-trap etc. In addition to this there are several ways to achieve enhanced mixing prior the SCR-catalyst and some more novel technologies to achieve high temperatures and high evaporation rates. This chapter explains some of the pros and cons with the various technologies and provides a small summary for each of the chosen concepts.

Chapter 4

This chapter provides a summary of the biomimetic field focusing on the previous research on the Bombardier beetle and why this small bug can be the inspiration source for the AUS-32 dosing technology.

Chapter 5

This chapter explains the patented μMist spray technology in more details and how this technology can be applied to various spray areas.

Chapter 6

This chapter explains the spray performance of the novel spray technology. Chapter 6 gives an overview of the experimental results obtained from the spray rig activities and explains the droplet sizes and mass flows generated by the injector for different chamber temperatures and internal injector timings.

Related Publications

Larsson P., Lennard W., Andersson Ö. and Tuneståł P. "A Droplet Size Investigation and Comparison Using a Novel Biomimetic Flash-Boiling Injector for AdBlue Injections", SAE Technical Paper 2016-01-2211, 2016, doi:10.4271/2016-01-2211.

Chapter 7

The first part of this chapter describes the experimental work conducted on a light-duty engine focusing on NOx-conversion and activation temperature achieved using the novel biomimetic doser. The second part of this chapter explaining a comparison between the same injector and a market leading technology using the same engine setup, focusing on mixing capabilities prior the SCR-catalyst.

Related Publications

Larsson P., Lennard W., Dahlström J., Andersson Ö. and Tuneståł P. ”NOx-Conversion and Activation Temperature of a SCR-Catalyst Whilst Using a Novel Biomimetic Flash-Boiling AdBlue Injecor on a LD Engine” SAE Technical Paper 2016-01-2212, 2016, doi:10.4271/2016-01-2212.

Larsson P., Ravenhill P., Larsson L-U. and Tuneståł P. ”SCR-Catalyst Utilisation and Mixing Comparisons using a Novel Biomimetic Flash-Boiling Injector”, ICEF2018-9763, ASME Conference Proceedings 2018.

Chapter 8

This chapter describes the experimental activities conducted on a HD-engine comparing the two described dosing technologies. This study focusing on the differences in NOx-reduction performance and ammonia slip reduction both using a flow restricted mixer plate and without one.

Related Publications

Larsson P., Ravenhill P. and Tuneståł P., ”NOx-Conversion Comparison of a SCR-Catalyst Using a Novel Biomimetic Effervescent Injector on a Heavy-Duty Engine”, SAE Technical Paper 2019-01-0047, 2019, doi:10.4271/2019-01-0047.

Chapter 9

This chapter concludes the results presented in this thesis.

Chapter 10

This chapter present a proposal on various future work needed for this concept in order to be introduced to the market.

Chapter 2

Diesel Engine Combustion and NOx Formation

2.1 Introduction

The history of combustion and specifically the internal combustion engine have been an important part of our society for thousands of years. Fire, the magic thing, that our ancestors used for cooking, to scare away dangerous animals as well as just use it for company and a place to warm themselves.

The first internal combustion engine ICE is basically the cannon [8]. The piston, even though this piston was a cannon ball, was pushed away by a rapid heat release from the ignition of gun powder. It took many years until someone came up with the idea to connect the flying piston to something and extract more useful work out of it. Christian Huygen used a working piston and heated up the working fluid with external combustion. But few people really understood what practical use this machine could have at the time. It took almost 40 years until Newcomen demonstrated that this new type of machine could be used to pump up water from mines. But due to the limited amount of flooded mines, the Newcomen engine didn't revolutionised the whole society until James Watt used an engine to produce rotary motion. This was a kick-off for the industrial revolution and the next hundred years new engines with higher power output were brought to the market, all with slightly different approaches. But none of these ideas are really used today due to the poor weight to power ratio. The real breakthrough, when it comes to ICE engines came 1876 [8]. This year Nicolaus Otto demonstrated the 4-stroke engine which is still the most used engine concept today. Otto employed spark ignition (SI), using a spark-plug in order to ignite the fuel charge. Another way to ignite the fuel and also one of the most common engines of today is with compression ignition, CI. Rudolf Diesel invented the first CI engine in 1892 and the development went fast from this point in time. Already 1897 the CI engine achieved 30.2% efficiency which was ground breaking at this time. Even though the CI engine is the most efficient engine on the market, the SI engine is still used to a large extent today [8].

There is mainly two large differences between the two concepts. SI runs with a stoichiometric fuel charge and uses a throttle to maintain the stoichiometric conditions for all speed and load cases. This has a negative effect on the gas exchange efficiency but it can utilise a three-way catalyst to treat the emissions efficiently. This engine and the connected exhaust after-treatment system is very simple and cheap to produce and that's the reason why this engine is still the most common engine for light-duty applications. The CI engine today is almost always operated with a lean fuel charge and compressed inlet air to increase the power. The diesel engine is not sensitive to knock which the gasoline engine is and therefore a diesel engine is capable of running with higher compression ratios. Looking at the thermal efficiency and the expression for the ideal cycle efficiency explain why this engine is more efficient [18].

$$\eta_t = 1 - \frac{1}{r_c^{\gamma-1}} \tag{2.1}$$

where (η_t) is the thermal efficiency, (r_c) is the compression ratio and if assuming a constant specific heat ratio (γ) the thermal efficiency increases with higher compression ratio.

2.2 4-stroke Diesel Engine

This section explains deeper why the diesel engine is the most common engine for heavy-duty vehicles and also why this type of engine needs extensive exhaust after-treatment system in comparison to the SI engine application. Even though this engine is more expensive to produce the normal customers of heavy-duty engine use the engine to increase their production in terms of delivering cargo from A to B and their main cost for this is fuel cost.

The 4-stroke diesel principle is described in Figure 2.1

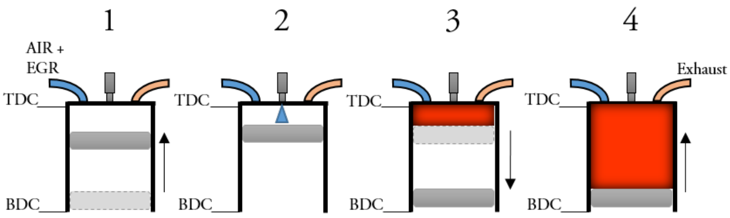

Figure 2.1: Working principle of a 4-stroke diesel cycle

The first stroke is the compression stroke where air and perhaps some residual gas EGR is compressed from bottom dead center, BDC, to top dead center, TDC. The second stroke is the fuel injection. This injection phase occurs close to TDC and with very high pressure the fuel is injected and starts to ignite by the hot air and EGR mixture. The third stroke is the work stroke in which the burned fuel raises the temperature further and the pressure from the heat release pushes the piston down towards BDC and work can be extracted. The fourth and last phase is the exhaust stroke when the piston moves from BDC to TDC and pushes the hot exhaust gases out, through the exhaust ports, towards the turbine of the turbo-charger. With the lean combustion this engine require treating the exhaust gases with other methods than the three-way catalyst. Compared to the SI engine, soot emissions needs to be treated with a diesel particulate filter, DPF. The focus of this thesis is on NOx emissions, the after-treatment of those and the CI engine as a potent contributor of NOx [18].

2.3 NOx-formation

NOx forms within the combustion cylinder in several ways. Usually four different mechanisms is used to describe the NOx production. The fuel mechanism are as the name describes, dependent on the fuel source. Different fuels have different amounts of nitric compounds. The type of fuel that is used during this investigation is MK1 which is also the most common type of diesel used in Sweden [23]. This fuel has a very low amount of nitric compound and it can be considered as negligible source of NOx formation [23] [32].

At lower temperatures below 1600°C the N_2O mechanism and the Prompt mechanism occur. The N_2O mechanism is a contributor if the fuel charge is very turbulent and lean [28]. The Prompt mechanism is rather the opposite and prominent at rich conditions [14].

In diesel engines where the combustion occurs at high temperatures with nitrogen and oxygen present, the Thermal mechanism is the most prominent source of NOx formation [37]. The NOx is mainly formed with the Zeldovich mechanism describing the two main reactions [39]:

$$N_2 + O \iff N + NO \tag{2.2}$$

$$N + O_2 \iff NO + N \tag{2.3}$$

There is also a third reaction occurring at near stoichiometric conditions [26] [30]:

$$N + OH \iff H + NO \tag{2.4}$$

Looking at the conceptual quasi-steady diesel combustion model by John Dec in Figure 2.2.

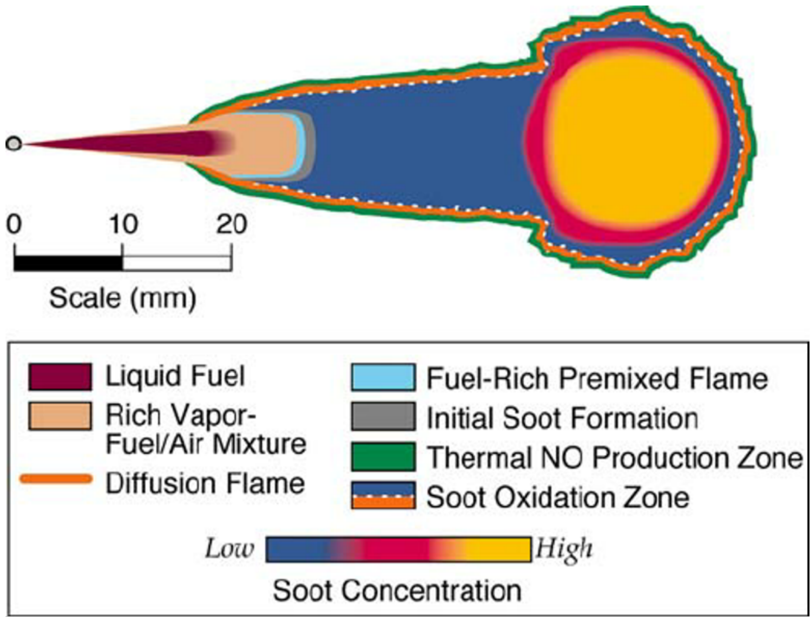

Figure 2.2: The quasi-steady diesel combustion flame, courtesy of John Dec [9]. The thermal NOx generation zone is the green outer layer in the flame.

The thermal NOx reactions occurs at a very thin line in the outer regions of the flame where the fuel to air ratio is almost stoichiometric. This can also be seen in the heat release. Figure 2.3 describes a typical heat release for diesel combustion.

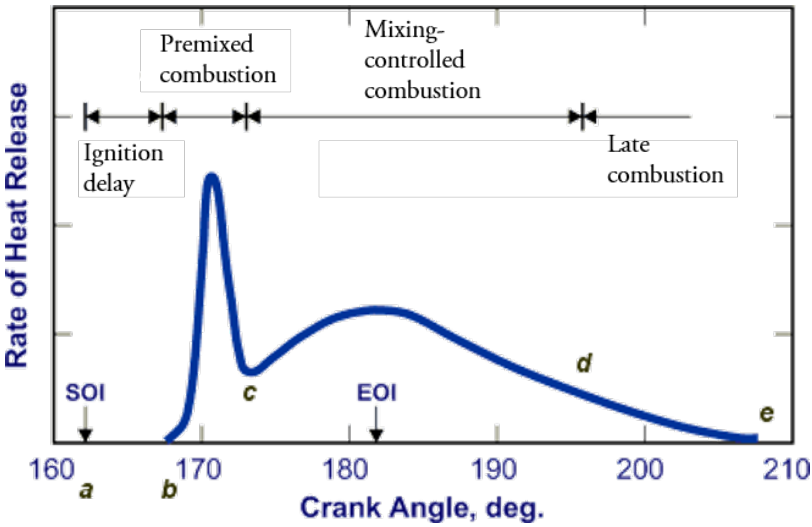

Figure 2.3: A typical diesel heat-release according to Heywood [18]. The major NOx formation process occurs during the mixing-controlled phase.

During the premixed phase, the combustion that occurs is very fuel rich and low amount of NOx is formed during this phase of the heat release. The major part of the NOx formation occurs during the mixing-controlled combustion phase where the conditions are suitible for the thermal NOx reactions to occur. This is unavoidable in diesel combustion and a NOx reduction method needs to be applied in order to treat the engine out NOx emissions.

Chapter 3

Overview of NOx Reduction Concepts

This chapter describes several technologies that reduce tail-pipe NOx emissions both with and without an external catalyst and some of the technologies can be combined which is rather common. The real problems with NOx emissions was first noticed in California in the 1950s when the problem with smog was at hand [16]. In Europe the first emission legislation EURO I came 1992 and the development of emission legislation over the years in Europe can be seen in Figure 3.1 [10].

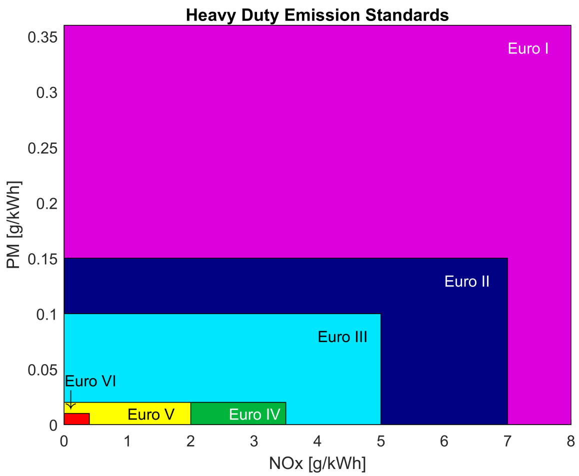

Figure 3.1: The European emission standards from Euro I to Euro VI [10]

Up until today the legislated NOx tail pipe emissions has been reduced from 8 g/kWh down to 0.4 g/kWh. The most common way to treat engine out NOx is by using EGR [34]. This is usually today used together with some additional technique described in this chapter.

Exhaust gas recirculation or EGR is as the name implies exhaust gases from the last cycle that are redirected back to the intake and with the high specific heat capacity of water and CO_2 the combustion temperature decreases and less NOx is formed. It has been shown that engine out NOx can be reduced by 50% for every 90K decrease at temperatures above 2100K [17]. But everything has a price and in this case the soot emission increases with lower λ-values and this trade-off is one of the reasons that this technique by itself is not feasible for the latest emission legislation.

3.1 Selective Catalytic Reduction

This method is the main focus of this thesis and later on how this technology can be enhanced compared to today's standard systems. This technology uses an additive such as AUS-32 that is dosed into the stream of exhaust gases up-stream of the SCR-catalyst. AUS-32 composition by standard is 32.5% Urea ($CO(NH_2)_2$) and 67.5% water [7]. This method is usually applied after the DPF & DOC and after the SCR catalyst an ammonia slip catalyst ASC is placed to treat the unwanted ammonia slip from the catalyst [33], see Figure 3.2.

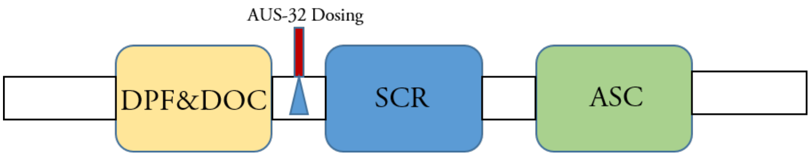

Figure 3.2: A schematic image over a typical heavy-duty emission system

The AUS-32 needs to be evaporated prior the catalytic surface and decomposed to form ammonia. The reactions that occur during this process is [6]:

$$CO(NH_2)_2 \longrightarrow NH_3 + HNCO \tag{3.1}$$

$$CO(NH_2)_2 + H_2O \longrightarrow 2NH_3 + CO_2 \tag{3.2}$$

The ammonia formed by these reactions reacts with the active substrate within the catalyst. There are several different substrates that can be used for this matter, such as vanadium oxides and copper zeolites, all with different characteristics based on the type of engine and exhaust temperatures [31] [36]. These substrates regardless of their composition have the purpose to enhance the NOx reduction reactions [21]:

$$4NO + 4NH_3 + O_2 \longrightarrow 4N_2 + 6H_2O \tag{3.3}$$

$$NO + NO_2 + 2NH_3 \longrightarrow 2N_2 + 3H_2O \tag{3.4}$$

$$2NO_2 + 4NH_3 + O_2 \longrightarrow 3N_2 + 6H_2O \tag{3.5}$$

Which of these reactions that occur depends on the NO/NO_2 ratio. Equation 3.3 is the dominant reaction if the NO/NO_2 ratio is greater than 1. The equation 3.4 is the most dominant if the NO/NO_2 ratio are equal or close to 1 and the third reaction 3.5 is the most dominant one if the NO/NO_2 ratio are less than 1.

One problem with SCR-technology and crude AUS-32 dosing is the risk of ammonia slip after the catalyst. This slip is today legislated to 10 ppm [10] and the excess slip needs to be treated with the ammonia slip catalyst so the tail pipe emissions contain a lower concentration than the legislated 10ppm. The ammonia slip catalyst uses the ammonia to react with oxygen to form nitrous oxide and water [15]:

$$2NH_3 + 2O_2 \longrightarrow N_2O + 3H_2O \tag{3.6}$$

The nitrous oxide is a very potent green house gas emission, 296 in CO_2 equivalent [19]. This emission is yet unregulated in Europe but since the US has started to look into this [35], it's just a matter of time until it is included even in the EURO emission legislation. So this is another incentive to enhance the performance and reduce the slip after the catalyst.

3.2 Lean NOx trap

Another common method of treating NOx emissions is the lean NOx trap or LNT. This method is particularly common on light-duty vehicles where the space is more limited compared to heavy-duty and this technique doesn't require a separate source of AUS-32. The method simply catches the NO and NO_2 molecules on a surface substrate and when the substrate starts to be saturated diesel is injected into the trap and the LNT is allowed to be regenerated during this process [38]. This method however starts to be replaced with SCR-technology on light-duty vehicles due to the more stringent legislation both on NOx emissions and also on the CO_2 addition of burning more diesel during the process.

3.3 Ammonia Storage and Delivering System

This technology, ASDS, is a rather novel technique that starts to appear on buses and in urban trucks. The technology can be retro-fitted to existing SCR-technology and instead of having liquid AUS-32 stored in a tank and dosed into the exhaust flow, a solid cartridge of ammonia is stored on the vehicle. This solid ammonia releases gasified ammonia directly into the exhaust flow and the decomposition reactions don't need to occur prior the catalyst and early tests have shown good conversion rates [22]. However this technology does need a completely different infrastructure around production of solid ammonia and also to supply large amounts to suppliers and costumers.

3.4 Heated Catalysts

There are also several different approaches to enhance the conversion rates of the catalyst and also decrease the time to light-off the catalyst. By simply having an external heater connected to the catalyst the time for the crude AUS-32 droplets to evaporate decreases and also the catalytic conversion can occur earlier. This method adds a couple of kW of electrical heating to the complete metal catalyst according to [13] [27].

Chapter 4

Bombardier Beetle

This chapter gives a brief introduction to the inspiration source for this project, the bombardier beetle, see Figure 4.1.

Figure 4.1: The Bombardier Beetle, courtesy of Swedish Biomimetic 3000 AB.

The bombardier beetle can be found on most of the continents in the world, stretching from South America to North America, Europe, Africa and all the way to Australia. In total there is more than 40 species all known by their ability to spray out a hot plume of a noxious chemical solution towards its attackers. The beetle uses it's abdominal tip as the firing barrel or nozzle and it can aim that with very high accuracy, rotating it more than a 270 degree pivot [27].

The beetle firing unit consists of two storage chambers, see Figure 4.2 with a thin membrane between, but with the ability to quickly mix the two reactants.

Figure 4.2: The two heart-shaped storage chambers that contains the two solutions within the Bombardier beetle, the image is from a dissection made by Eisner [29].

The first chamber contains hydrogen peroxide and hydroquinone and the other contains several enzymes. The enzymes react with hydrogen to form oxygen and water and the oxygen then reacts with the hydroquinone to form benzoquinone. This reaction is very exothermic and temperatures up to 100°C can be achieved during a very short period of time before the pressure relief valves pop's open by the increased pressure due to the temperature and formation of oxygen [29].

Chapter 5

The Novel Biomimetic Injection System

This chapter describes the novel biomimetic injector system in more detail. The injector is inspired by nature and the bombardier beetle in particular.

5.1 Introduction

Previous studies have shown an enhancement in reducing droplet sizes using the μMist technology [3]. Initially this novel biomimetic injector was developed by the University of Leeds with the support from Swedish Biomimetic 3000 and then by the company themselves. At this time the focus of the development was towards using gasoline as the working fluid. The engine testing was performed at the Loughborough University focusing on port-fuel injection in a Lotus light-duty engine [4]. One conclusion from the particular study was that the new technology produced very small droplets of gasoline that quickly evaporated in the intake manifold and these findings lead in the end to the discussions of injecting AUS-32 into the stream of exhaust gases to possibly enhance the evaporation and mixing capabilities for SCR-catalyst technology.

5.2 μMist Injector Technology

The earlier studies lead to a patented injector system and a schematic of that can be seen in Figure 5.1.

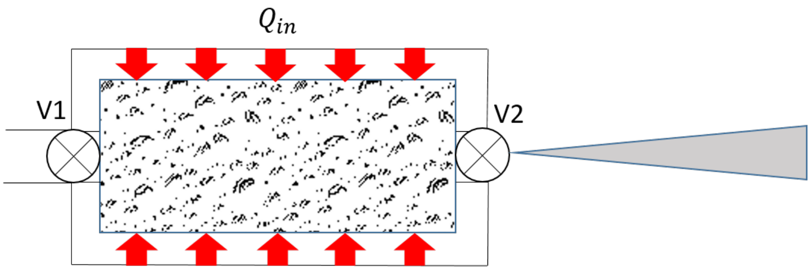

Figure 5.1: A schematic image of the μMist injector technology. The figure describes the constant volume chamber, the mass flows through the chamber and the heating of the same.

The working principle of this system can be divided into four stages and these combined make a full cycle. The first stage can be described as the inlet stage or filling stage. During this stage V1 is kept open during the time T1 and the fluid is pumped into the injector by an external feed pump. The required pressure during this operation is set by the remaining chamber pressure that needs to be overcome with the pump pressure. The second stage is the heat-up stage. During T2 both V1 and V2 are closed and the liquid is contained in the closed constant volume chamber and heated up to the target temperature. The minimum required temperature is set by the pressure of the outside environment that the fluid is sprayed into. This fluid needs to be heated to a temperature such that the saturated vapor pressure (SVP) exceeds the ambient pressure.
At the time of start of injection (SOI) the cycle enters the next stage during T3. During this stage V2 is open and the injector expels a plume of small droplets into the target environment. An example of the spray can be seen in Figure 5.2.

This image is captured with a high speed camera and the speed of the droplets was calculated, by tracing a single droplet, to 60 m/s. The next stage T4 is the time between the previous cycle and the next cycle. This stage can be used to add an additional degree of freedom for frequency control. Figure 5.3 describes the different stages.

In order to certify and fully understand the driving factor (DF) of the injector a series of different spray tests with AUS-32 were conducted with different chamber temperatures. Figure 5.4 shows the results from this investigation.

All the measured pressures within the constant volume chamber were recorded at the time of SOI when T2 was finished. The plotted SVP of water was extracted

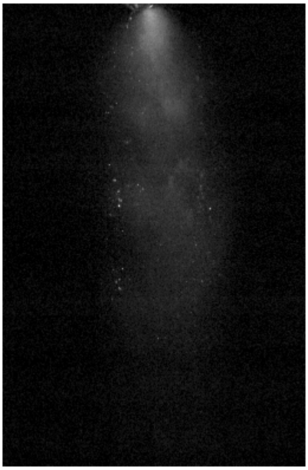

Figure 5.2: A fully developed spray plume at 170°C chamber temperature captured at 60000 fps.

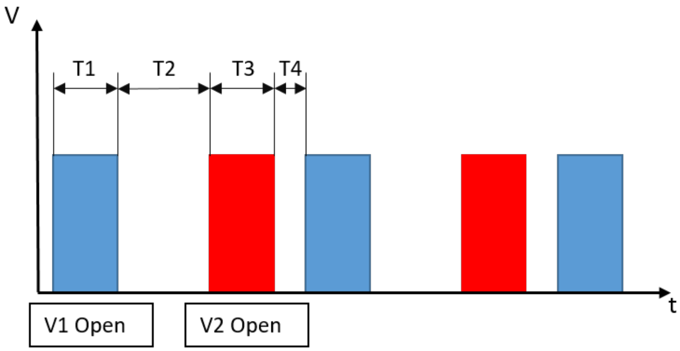

Figure 5.3: A schematic illustration of the injector timings that together concludes one injector cycle. The x-axis describing time and y-axis is the voltage to the solenoid valves.

from the thermodynamic property data tables [5].
As one can see there is fluctuations between the measurement data and the theoretical SVP data for each temperature. This is mainly noticeable for the lower temperatures during the investigation. The reason for that is the feed pressure. During low chamber pressures <6bar the influence of the feed pressure is larger and the resulting chamber pressure will be higher. The big outliers can be explained simply by measurement error and that the temperature control at this early stage was ±5°C. Another reason for pressure fluctuations is internal injector timings. The resulting fluid to vapor ratio within the constant chamber varies with inlet and outlet timing and this has been shown to have an effect on the total chamber pressure.

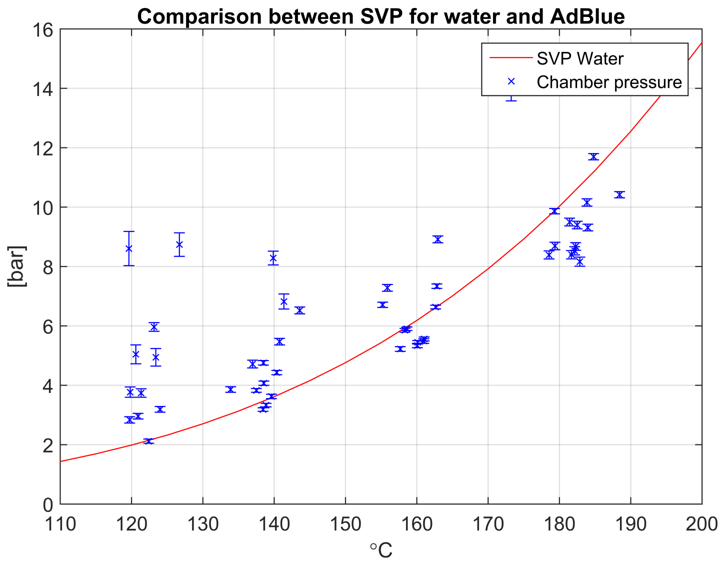

Figure 5.4: A comparison of the measured chamber pressure for different chamber temperatures. The x-axis displays the measured temperature and the y-axis the absolute pressure in bar.

Chapter 6

μMist Spray Investigation

This chapter includes the droplet size investigation performed in order to evaluate the potentials of the novel injector technology, described in more details in Chapter 5.

6.1 Rig Setup

The spray rig setup is shown in Figure 6.1

During this study a total of 3 different dosing units have been analysed and

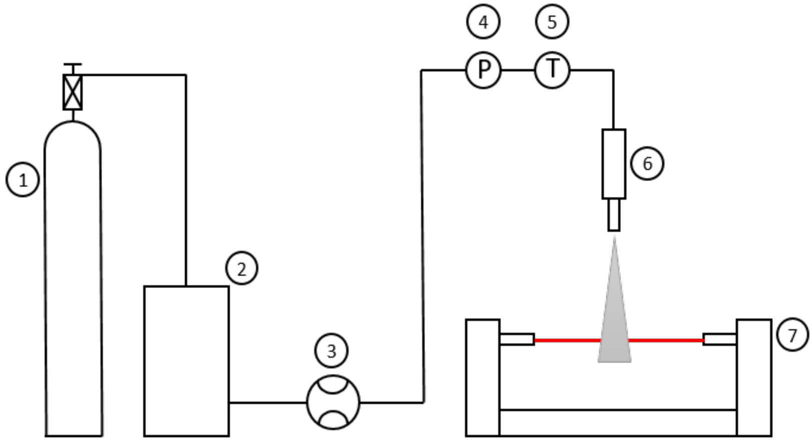

Figure 6.1: A schematic image of the spray rig setup including the (1)Gas Canister (2)AUS-32 Supply (3)Flow Meter (4)Inlet Pressure Sensor (5)Inlet Thermocouple (6)Dosing Unit (7)Droplet Size Analyser

benchmarked to each other. The first injector tested was the patented μMist injector. The second one was a modified version of the same unit but with the exception that the inlet valve was removed and then the injector acts as a "normal" heated doser. The third injector tested was the 3-hole market leading injector.

The supply line of fresh AUS-32 to the dosing unit is pressurised by Nitrogen. A high pressure piston-displacement flow meter is used to measure the injected mass flow, with the accuracy of $\pm0.2\%$. Type K thermocouples were installed both internally in the doser and on the fresh supply line. In total, 3 pressure sensors were used in the setup, one absolute pressure sensor on the supply line and two on the dosing unit. The first, a piezo-electric sensor, for fast sensing of in-chamber pressure fluctuations and the other absolute sensor for pegging the fast sensor. All measurement signals were collected and displayed through National Instrument software and hardware measuring the analogue signals with 20kS/s in order to achieve high accuracy. A Malvern Spraytec system using laser diffraction method was used to sample and display real-time measurements of droplet sizes and histograms of the spray plume.

6.2 Methodology

The methodology for this test aims to investigate the different exit times T_3 and different chamber temperatures in order to look at the spray performance, droplet sizes, mass flows and droplet size distribution. The different tested inputs for the novel dosing unit can be seen in Table 6.1.

Table 6.1: The different dosing unit inputs for the μMist injector

Case #			[ms]	
	T_1	T_2	T_3	T_4
1	10	20	5	1
2	10	20	10	1
3	10	20	15	1
4	10	20	20	1
Case number 1-4 were repeated 12 times each				
49	10	50	20	1
50	50	20	20	1

All the above settings were repeated 3 times, giving a total of 12 test points on the different temperatures, (130°C, 150°C, 170°C and 190°C). Case number 49 represents the behaviour if a long heating time is used and case number 50 a long filling time. This is to ensure that the chamber liquid is homogeneously tempered and the chamber is completely filled respectively. The inlet pressure was kept at 9 bar.

To quantify the performance of the new AUS-32 injector technology the investigation included 3 other techniques or injectors to benchmark against. One of these were a market leading standard solenoid injector and the other two were, the air-assisted and the regular heated injector.

The tested solenoid injector is tested at 9 bar inlet pressure and with the same "peak and hold" signal as for the μMist injector. The manufacturer has stated in their data sheet for the injector that its delivers droplet sizes of 75 μm in SMD.

For the benchmarking tests the following operating points were used for all the tested injectors, see Table 6.2.

Table 6.2: The benchmarked operating points

Case #	**μMist injector and the heated injector**					**Market leading injector**				
	T_1	T_2	T_3	T_4	°C	T_1	T_2	T_3	T_4	°C
1	10	20	5	1	170	10	20	5	1	25
2	10	20	10	1	170	10	20	10	1	25
3	10	20	15	1	170	10	20	15	1	25
4	10	20	20	1	170	10	20	20	1	25

6.3 Results

The results section is divided into two parts. The first part describes the performance of the μMist injector and the second part describes the differences between the injectors in the bench-marking investigation.

6.3.1 μMist injector performance

The AUS-32 mass flow for the different tested cases is described in Figure 6.2. Overall there is mainly two settings that influence the ejected mass, the operating temperature and the inlet valve opening time.

The mass flows is independent of temperatures up to 170°C, but if the temperature exceeds that the mass flows decreases. This is due to the SVP of the liquid, Figure 5.4, and for temperatures higher than 170°C the injector is not able to re-fill because the SVP increases above the feed pressure of 9 bar. So if the injector needs to have a higher chamber temperature the feed pressure

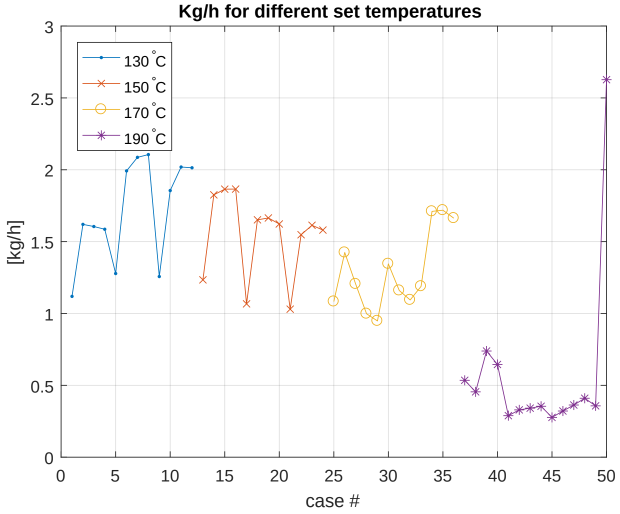

Figure 6.2: The total mass flows for the different tested temperatures for all the cases. The X-axis describes the different cases and the Y-axis the measured mass flows in [kg/h].

needs to be increased. One can see a variation in mass flows for every specific temperature depending on the outlet time up to the point where the chamber pressure equals the ambient pressure and if the needle is still open when the difference is small, case 3 and case 4, there is no pressure to force the liquid out.

For the last case number 50 the feed pressure was increase to 16 bar together with a long inlet valve opening time in order to show the refilling issue and the mass flow increased drastically accordingly.

The droplet sizes were measured during every set of experiments and the results for Dv10 can be seen in Figure 6.3.

The meaning of Dv10 as a term is that 10% of the volume contains droplets smaller than the specified value. Figure 6.3 describes the clear trend of the μMist performance. Lower temperatures has a tendency of creating larger droplets and when the temperature increases the effect of flash-boiling increases and the rapid expansion results in significantly smaller droplet sizes.

Another term commonly used when presenting droplet sizes and sprays is the Sauter Mean Diameter SMD, especially when describing evaporative sprays. The reason is that SMD describes the spray's volume to surface area and is defined as the diameter of a sphere that has the same volume/surface area as the collection of particles in the spray [25].

Figure 6.4 describe the SMD for all the tested cases. The trend for the presented

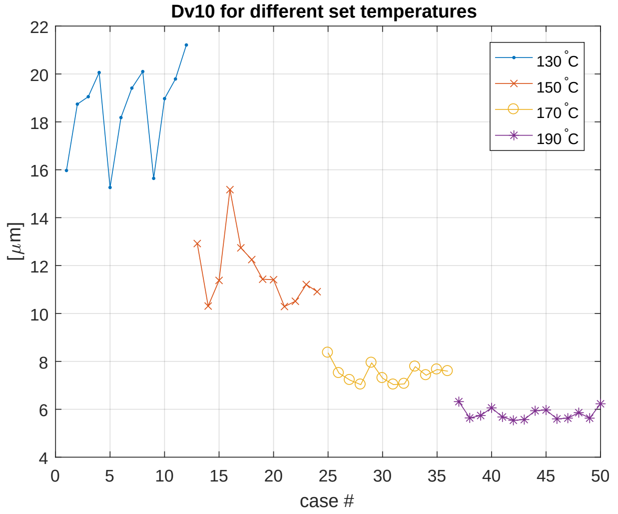

Figure 6.3: The droplet sizes presented in Dv10 for the different tested temperatures for all the cases. The X-axis describes the different cases and the Y-axis the measured droplet sizes in [μm].

SMD values is the same as for the Dv10. The results show that the μMist delivers approximately 10μm in SMD for the 190°C case.

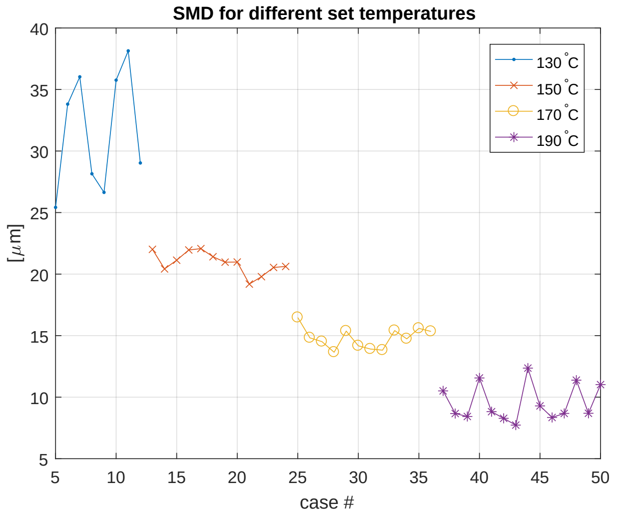

Figure 6.4: The droplet sizes presented in SMD for the different tested temperatures for all the cases. The X-axis describes the different cases and the Y-axis the measured droplet sizes in [μm].

One can also see in both Figure 6.3 and Figure 6.4 that the droplet sizes varies with different outlet times, T_3 for the lower temperatures and this is due to the strength in droplet break-up. For the lower temperatures the droplet break-up is weaker and the smallest droplets are delivered initially during T_3 and if the injector is kept open for a longer time the smaller droplets are followed by larger droplets for the remaining time. For higher temperatures this effect is smaller since the smaller droplets can be delivered during a longer period. One can rather see that the effect is inverted so that initially when the needle opening is too narrow between the needle and the seat, the small droplets can instead coalesce and form larger droplets.

This is more apparent from the droplet size distributions, Figure 6.5 and Figure 6.6.

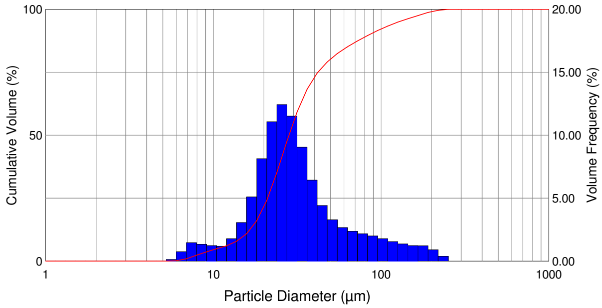

Figure 6.5: The droplet sizes distribution for case 5 with short T_3 and 130°C. The red line shows the cumulative volume in [%] in the left Y-axis. The height of the bars shows the Volume Frequency in [%] on the right Y-axis. The X-axis represents the particle diameter in [μm].

For the lowest temperature and the shortest T_3 there is a small peak with very small droplets but the main peak is located at droplet sizes from 10-50μm followed by a rather large tail of larger droplets. This interesting feature of the μMist effervescent injector can be seen in Figure 6.6.

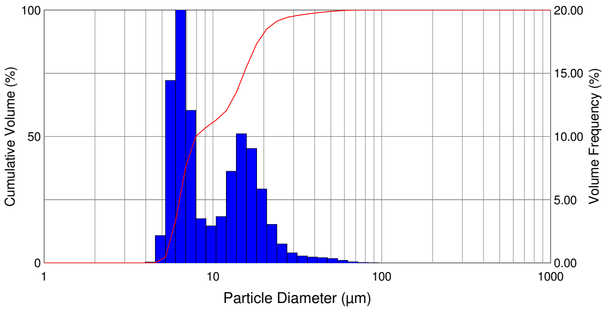

Figure 6.6: The droplet sizes distribution for case 41 with short T_3 and 190°C. The red line shows the cumulative volume in [%] in the left Y-axis. The height of the bars shows the Volume Frequency in [%] on the right Y-axis. The X-axis represents the particle diameter in [μm].

The high temperature shifts the large peak towards smaller droplet sizes and more than 50% of the cumulative volume consists of droplets $< 10\mu$m. This first peak is the main effect of the flash-boiling phenomenon which creates very small droplets. But when these droplets travel from the chamber through the narrow nozzle, some of the droplets coalesce into larger droplets and this describes the second peak.

To quantify the results and the novel injector technology, the data has been compared to a few competitive technologies. In order to get a good comparative data set the same injector timings are used for the different tested technologies, as seen in Table 6.2. All other inputs have been kept constant, except the operating temperature for the market leading technology which was kept at room temperature, 25°C.

The mass flow comparison between the injectors can be seen in Figure 6.7.

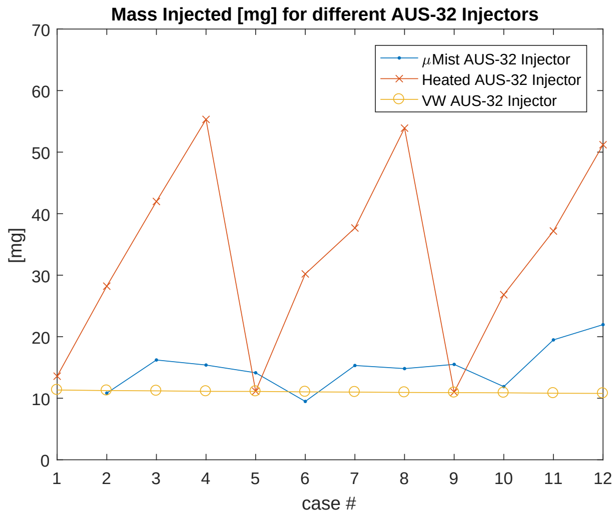

Figure 6.7: The injected mass per cycle for each of the tested injectors. The x-axis describes the different tested cases from Table 6.2 and the y-axis the mass injected in [mg].

The injected mass per cycle changes depending on the tested technology. The heated injector, with only the outlet solenoid working, has the expected linear behaviour depending on opening time T_3. The market injector had a constant injected mass regardless of actuation time with the "peak and hold" shaped 5V signal. For the novel technology the amount is increasing from 5 ms to 10 ms but then the flow remains constant for the remaining timings. The total flow rate will therefore be frequency controlled for the set opening time.

Figure 6.8 shows the droplet sizes of the tested injectors including the presented value of 15μm in SMD from the air-assisted technology.

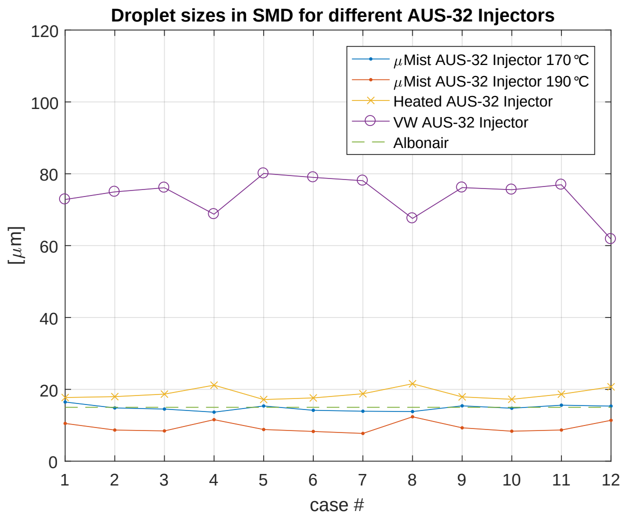

Figure 6.8: The droplet sizes calculated in SMD for the different tested injectors. The x-axis describes the different tested cases from Table 6.2 and the y-axis the SMD droplet sizes in [μm].

Overall the droplet size is rather constant for each single technology but differs significantly between the market leading technology and the more novel ones. The smallest recorded droplet sizes is projected to evaporate faster and mix well with the hot exhaust gases, was with the μMist dosing unit.

6.4 Summary

With laser diffraction method and piston-displacement flow metering a series of results have been acquired and analysed for several different dosing techniques. The main conclusion from this study was that droplet sizes of below 10μm in SMD have been measured with the novel μMist effervescent doser. To compare this result with the other tested dosing techniques, the μMist doser delivered 33% smaller droplets on average compared to the other novel technologies and up to a 87% size reduction compared to the market leading standard.

Chapter 7

Light-Duty Testing and Catalyst Distribution

This chapter summarises the light-duty activities conducted with the μMist dosing system. It includes both the initial NOx-conversion and activation temperature tests together with the SCR-catalyst utilisation and mixing comparison between the μMist and the market leading 3-hole doser.

7.1 Rig Setup

The investigations described in this chapter have been conducted on a Volvo VED 4 engine, which is a 4-cylinder production diesel engine from Volvo Cars, see Figure 7.1.

During these studies normal Swedish MK1 diesel has been used in the 2-liter engine. Since the engine is a production engine installed in the test facilities at Lund University a couple of modifications have been made. The turbo-charger has been removed and replaced with the compressed air line from the building. The reason is to enable full control of the intake pressure. The standard ECU has been replaced with the in-house LabVIEW software, installed in most of the test cells. The engine control hardware is a PXI-system to enable fast sampling at 0.2 CAD. All thermocouples, pressure sensors and injector drivers are controlled and monitored by the same system. A complete engine specification can be seen in Table 7.1.

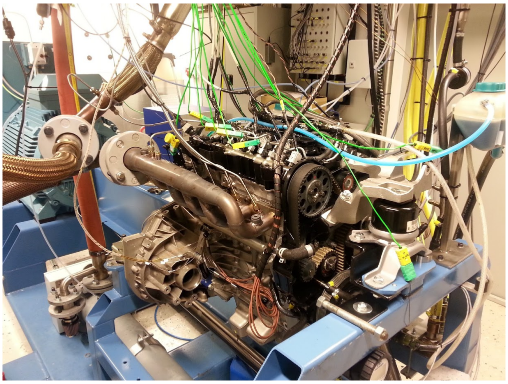

Figure 7.1: The engine setup describing the Volvo VED4 engine.

Table 7.1: Volvo VED4 engine specifications

Engine Type	Volvo VED
Displacement [cm^3]	1969
N° of Cylinders	4
Compression Ratio	15.8
Bore x Stroke	82 x 93.2
Valves per Cylinder	4
Diesel fuel system	Denso G4S
Max Power [kW]	133
Max Torque [Nm]	400

7.1.1 SCR-Catalyst

In total two different SCR-Catalysts have been used during these studies. The catalyst used during the activation temperature study was a Vanadium based catalyst. For the utilisation and mixing comparison study a standard VW-Crafter model year 2011 catalyst was used. The dimensions of both catalysts can be seen in Table 7.2

Table 7.2: SCR-Catalyst specifications

Vanadium Catalyst		**VW-Crafter 2011**	
Length [m]	0.3	Length [m]	2 x 0.13
Diameter [m]	0.4	Diameter [m]	0.15
Volume [m^3]	0.0377	Volume [m^3]	0.0046
Pipe Diameter [m]	0.06	Pipe Diameter [m]	0.06

Apart from the two different catalysts a measurement probe unit has been used during the mixing study. This probe was custom made for the purpose of measuring exhaust gases at 17 different locations and located directly downstream of the catalyst, see Figure 7.2.

Figure 7.2: The exhaust probe unit included the 17 different locations for individual exhaust probe measurement.

The guide pipes, in which the measurement probes are installed, are close coupled to the catalyst grid in order to prevent exhaust gases slipping through. Exhaust measurement was conducted with an AVL AMA I60 system. Ammonia slip was measured with a Siemens LDS6 system, which uses a diode laser in order to analyse the ammonia in the exhaust stream. To ensure precise measurements a 1.5 meter pipe was installed after the catalyst and the Siemens system is installed at each end of that pipe. Overall exhaust measurements were taken both directly before and directly after the catalyst. In total 3 different thermocouples measuring the catalyst temperature and the ammonia measurement calibration temperature. The complete catalyst installation can be seen in Figure 7.3.

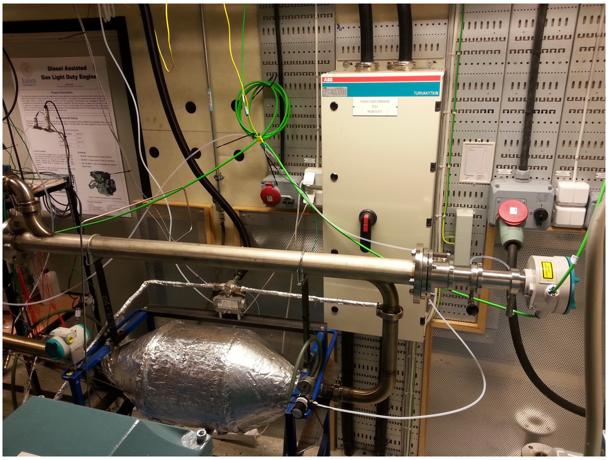

Figure 7.3: The complete assembly of the catalyst and the ammonia slip measurement pipe located on top of the catalyst. The dosing units is located in the bottom left corner of the figure.

7.2 Methodology

The overall aims for these studies was to investigate the performance of the novel AUS-32 dosing unit on a light-duty engine focusing on conversion rates, ammonia slip, activation temperature and mixing capabilities. To quantify the results the collected data has been analysed and compared with data generated with the 3-hole market leading standard doser for most of the tested conditions.

The engine operating conditions were kept constant throughout both studies, which can be seen in Table 7.3.

Table 7.3: The operating condition for the VED4 engine

Engine Speed [rpm]	1500
Common rail pressure [bar]	1600
Fuel flow [g/s]	1.42
Exhaust flow [kg/h]	145
Exhaust temperature [^{c}ircC]	340
Power [kW]	25
IMEP [bar]	11.2-11.5
EGR [%]	0-4

The initial activation temperature was conducted with the bent inlet pipe configuration, see Figure 7.4.

The mixing study was conducted with two different pipe settings together with a mixer plate installed between the pipe and the catalyst for some of the cases. The inlet pipe settings for the mixing study can be seen in Figure 7.5

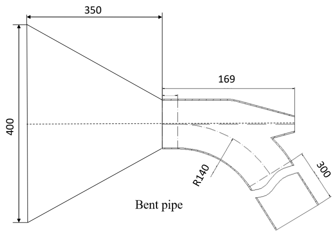

Figure 7.4: The bent inlet pipe configuration used on the Vanadium catalyst during the activation temperature test.

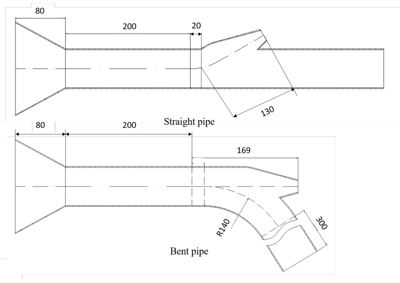

Figure 7.5: The bent inlet pipe configuration used on the VW Crafter catalyst during the mixing investigation.

In total 8 different setups were investigated, 4 of these with the novel AUS-32 doser and 4 with the 3-hole market leading doser. Each of the dosers are tested against the different pipe setups and also with or without a flow restricted mixer plate. The different test configurations are summarised in Table 7.4.

Table 7.4: The different tested cases summarised for the mixing comparison investigation

Setup N°	Pipe and injector setting	Case N°
1	μMist injector, Bent pipe, without mixer	1
2	Bosch injector, Bent pipe, without mixer	
3	μMist injector, Straight pipe, without mixer	2
4	Bosch injector, Straight pipe, without mixer	
5	Bosch injector, Straight pipe, with mixer	3
6	μMist injector, Straight pipe, with mixer	
7	μMist injector, Bent pipe, with mixer	4
8	Bosch injector, Bent pipe, with mixer	

The procedure in order to achieve a good comparison was that the AUS-32 dosing was initiated when the engine operation was considered stable and the catalyst temperature reached 300°C. The conversion measurement was initiated when the ammonia slip reached 5ppm and data was collected during the 150 consecutive cycles. This was repeated 17 times covering the surface of the catalyst, giving a total of 152 test points plus 8 overall conversion and ammonia slip tests.

7.3 Results

The initial results presented in this section focusing on the activation temperature and the overall conversion for an AUS-32 flow rate sweep. Initially the engine was set to producing high NOx output and high exhaust temperature.

The dosing strategy at this point was to start at a high flow rate and consequently decrease it to find the sweet spot of the lowest possible dosing rate resulting in the highest possible conversion rate for this particular setting. Continuing with a slight boost in intake pressure the exhaust mass flow increased together with a slight decrease in NOx output. The dosing strategy was instead to start at very low mass flow and investigate the lowest possible AUS-32 dosing with the highest conversion rate.

The exhaust mass flows during this investigation and the NOx output can be seen in Figure 7.6 and Figure 7.7 respectively.

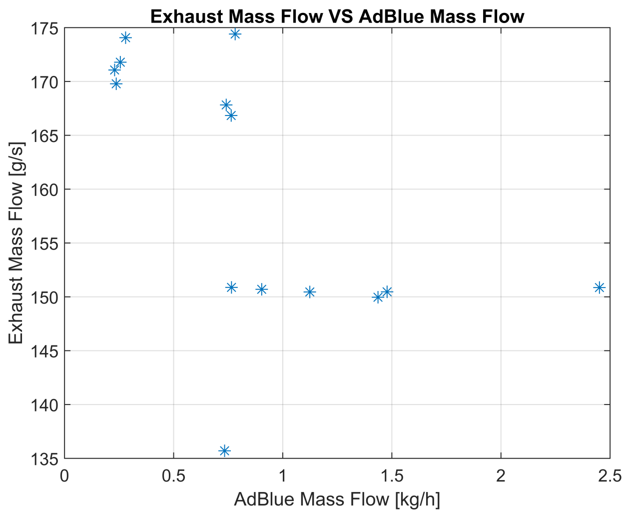

Figure 7.6: The engine out exhaust mass flow during the initial testings. Each of the plotted markers represent the measured flows and plotted towards the corresponding AUS-32 mass flow used during that experimental point. The exhaust mass flow in [kg/h] is presented on the y-axis and the x-axis represents the current AUS-32 mass flow.

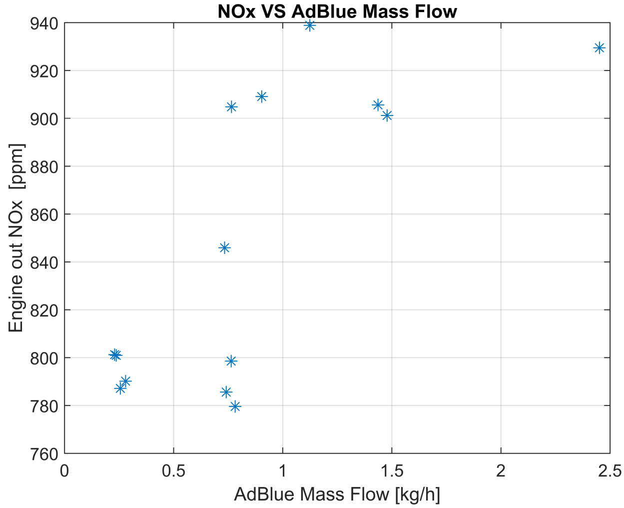

Figure 7.7: The engine out NOx plotted towards each of the target AUS-32 mass flows used during the investigation. The Y-axis describes the measured NOx concentration without any AUS-32 dosing. The x-axis represents the current experimental point expressed in AUS-32 mass flow.

The catalyst temperature during these two steps were 375° for the higher NOx output and 345° for the lower NOx output. Figure 7.8 shows the NOx conversion efficiency according to expression 7.1

$$\eta_{NOx} = 1 - \frac{NOx_{after}}{NOx_{before}} \tag{7.1}$$

This result is without any flow restricted mixers and the injector is positioned 450mm away from the frontal surface area of the catalyst. The conversion rate increases quickly up to nearly 100% for the high output NOx and remains constant throughout the high dosing points. Figure 7.9 describes the tailpipe NOx converted into the regulated unit of [g/kWh].

This indicates that the challenge with AUS-32 dosing at the tested condition with high catalyst temperature is to match the dosing rate to current NOx output, if only tailpipe NOx is considered. The emitted tailpipe NOx during this investigation rapidly decreased below 0.4 g/kWh and remained below that certain value during the remaining higher dosing rates.

The dosing strategy becomes more challenging when the ammonia slip needs to be taken into account. Excess AUS-32 dosing results in a slip of ammonia into the exhaust stream after the catalyst. Figure 7.10 describes the ANR for this particular test and this value explains the ammonia to NOx ratio and this is

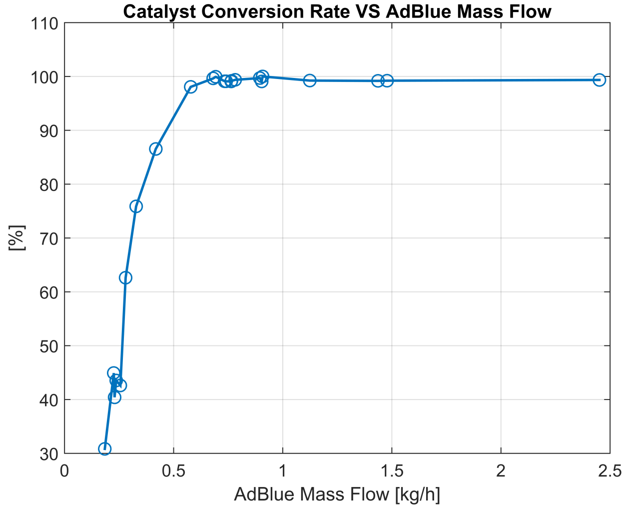

Figure 7.8: The SCR catalyst conversion efficiency between the measured SCR-outlet NOx and the inlet NOx emission. The x-axis shows the corresponding dosing rate for that particular conversion rate.

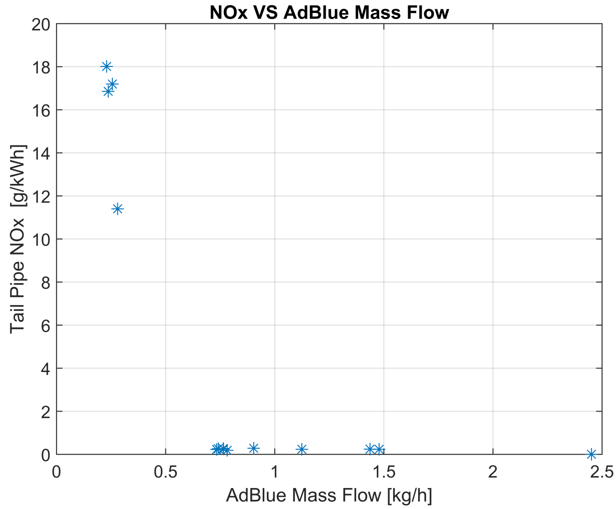

Figure 7.9: The SCR catalyst outlet NOx emissions calculated as the regulated [g/kWh]. The X-axis describes the corresponding AUS-32 mass flows for each of the plotted experimental point.

usually used to find a window where both the tailpipe NOx and the ammonia slip is at their minimum.

The 10ppm ammonia slip limit during this experiment was at an ANR value between 0.5 to 0.6 which is a bit low. However this can indicate that there was a bit of ammonia storage build up inside the catalyst.

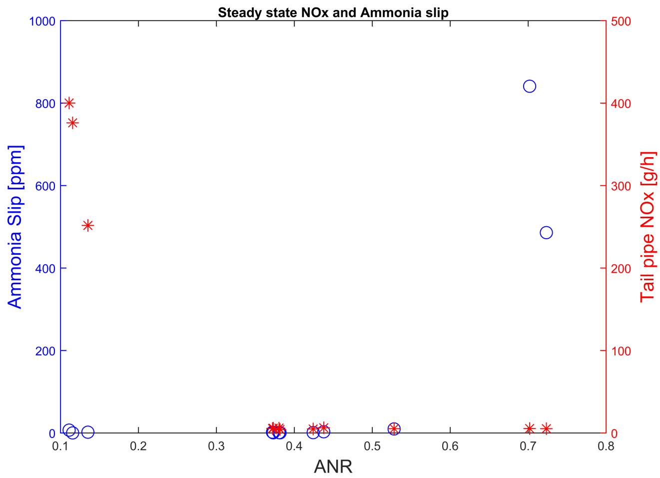

Figure 7.10: The ammonia slip and the tail pipe NOx emissions VS. the resulting ANR ratio.

Another important factor for good overall NOx conversion is the activation temperature at the catalyst itself. During the time of this study the limit of when to initiate the dosing into the exhaust stream was around 220°C but if this limit could decrease with maintained conversion efficiency a lot more NOx could be converted during the cold-start period of the vehicle. To investigate the performance of the novel injector, the engine was started from cold and when the NOx emissions reached the target value the AUS-32 was initiated. The dosing rate during this test was 0.9 kg/h of AUS-32 mass flow. Figure 7.11 shows the conversion rate during the engine start-up phase when the dosing was initiated.

The NOx-conversion exceeds 90% already at below 200°C and increases up to nearly 98% conversion just above 200°C. This result indicates that the small preheated droplets of 20μm in SMD enhance the evaporation and mixing prior the catalyst and enable good conversion already at low exhaust temperatures.

To further investigate the difference in mixing capability for this novel injector technology a series of tests were conducted on the same engine and catalyst setup with maintained operating conditions. The reason is that the results can be comparable with the activation temperature study. The hypothesis was that the small preheated droplets evaporate faster and enhance the mixing process prior the catalyst surface.

Figure 7.12 describes the results for the two different tested dosers injected into

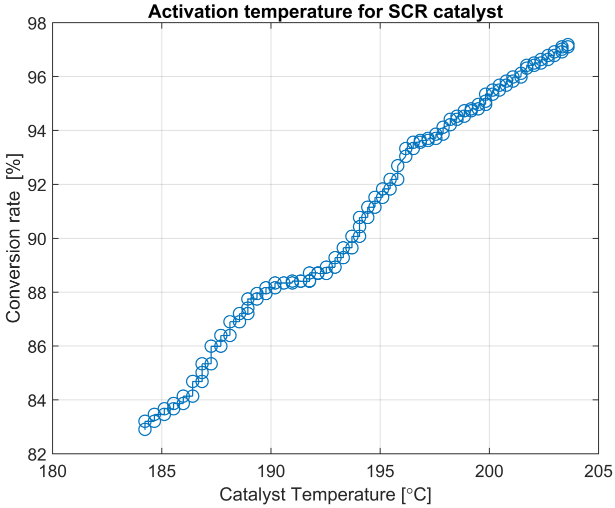

Figure 7.11: Continuous temperature measurements averaged over the catalyst during engine start-up. The y-axis presents the catalyst conversion rate and the x-axis shows the current temperature. The target dosing rate during the test was 0.9kg/h.

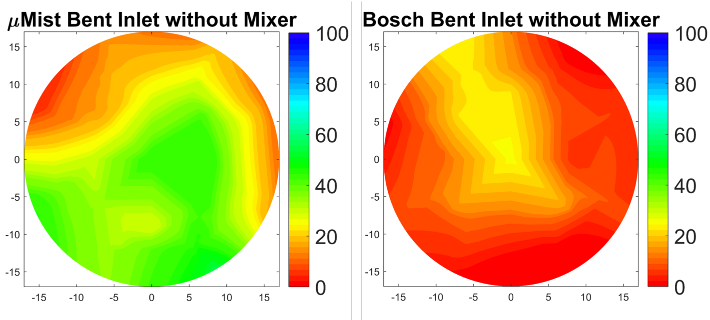

Figure 7.12: The conversion rates for the novel biomimetic injector(left) and the market leading technology(right) injecting into the bent pipe configuration without a mixer plate installed(Case 1). The orientation in the picture is the top section in the figure representing the upper surface on the catalyst.

the bent inlet pipe and without the market mixing plate installed. The novel injector (left figure) achieves a much better conversion over the surface compared to the market leading injector. There is a larger collection of droplets on the mid and lower area due to the exhaust flow structures. There is a clear trend that the small droplets follow the stream of exhaust gases in a larger extent compared to the larger droplets in the right figure. This is more noticeable comparing with the results from the straight pipe test, Figure 7.13.

Here the flow structures of the exhaust gases are less interfered prior the injection location resulting in a more equal result for the two technologies. However the

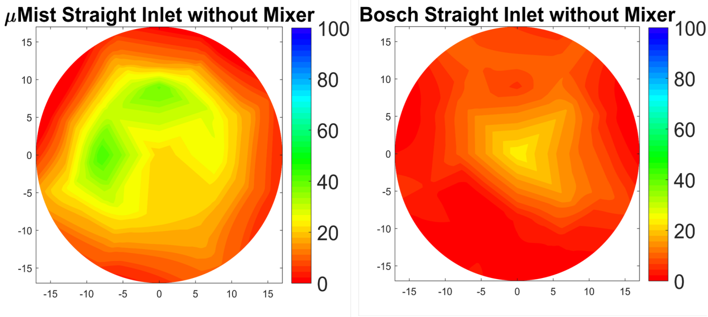

Figure 7.13: The conversion rates for the novel biomimetic injector(left) and the market leading technology(right) injecting into the straight pipe configuration without a mixer plate installed(Case 2). The orientation in the picture is the top section in the figure representing the upper surface on the catalyst.

novel injector still evaporates the droplets far better prior the catalytic surface, which can be seen in a higher conversion rate in the middle section of the catalyst. Injection at an angle from the side and with the long straight flow structure tends to be disadvantageous to the overall conversion result and the mixing process.

Figure 7.14 shows the result of the same pipe setting but with the flow restricted mixer plate installed. This setup is the standard setup for the market leading doser in terms of flow structure prior the catalyst.

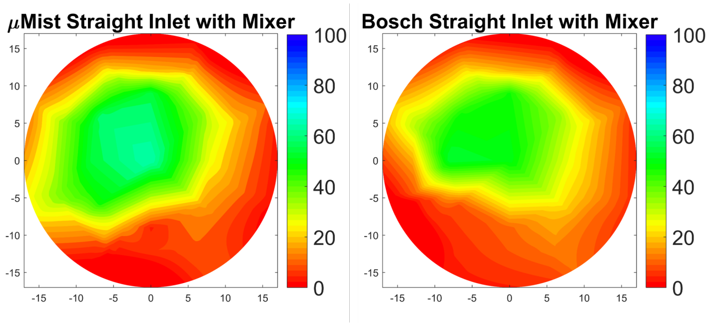

Figure 7.14: The conversion rates for the novel biomimetic injector(left) and the market leading technology(right) injecting into the straight pipe configuration with a mixer plate installed(Case 3). The orientation in the picture is the top section in the figure representing the upper surface on the catalyst.

The two technologies are more comparable to each other with this setup and the majority of the AUS-32 is collected in the middle section of the catalyst. This setup is the standard setup for the market leading doser. The last tested setup is the bent inlet pipe with the mixer plate installed, see Figure 7.15.

The overall performance for both dosers are greatly enhanced if compared to the previous results. This indicates that the mixing plate enhances the mixing

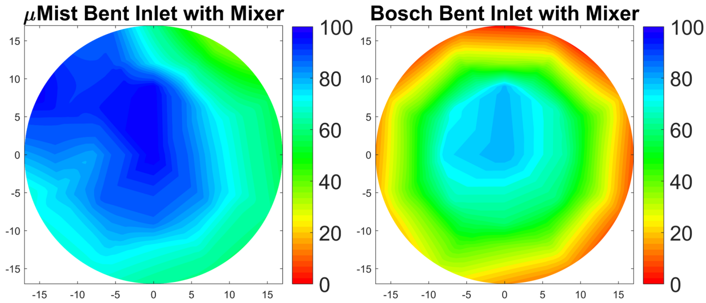

Figure 7.15: The conversion rates for the novel biomimetic injector(left) and the market leading technology(right) injecting into the bent pipe configuration with a mixer plate installed(Case 4). The orientation in the picture is the top section in the figure representing the upper surface on the catalyst.

process up-stream of the catalyst and the trade-off between the increased back-pressure and the increased conversion should be taken into account even with the novel injector technology. Another indication of the enhanced mixing performance is the swirling motion noticeable in the left figure and that the droplets tends to follow the exhaust flow structures better with the smaller droplets.

The overall conversion can be seen in Figure 7.16 for both technologies.

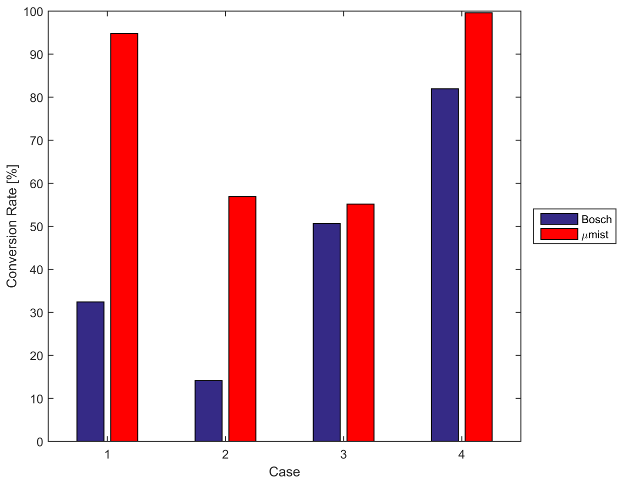

Figure 7.16: The overall conversion rates for all the tested cases. The different color coding represent the two different dosers. The x-axis describes the different cases and the Y-axis the corresponding conversion rates.

The up-stream droplet evaporation and mixing capabilities have a large impact on the overall conversion rate and the differences are more significant when the mixer plate was removed from the setup. The increase in turbulence induced by the bent pipe structure enhances the performance, more significantly if the spray plume is highly dispersed with small droplet sizes.

The overall ammonia slip was measured for all tested conditions and the results are presented in Figure 7.17.

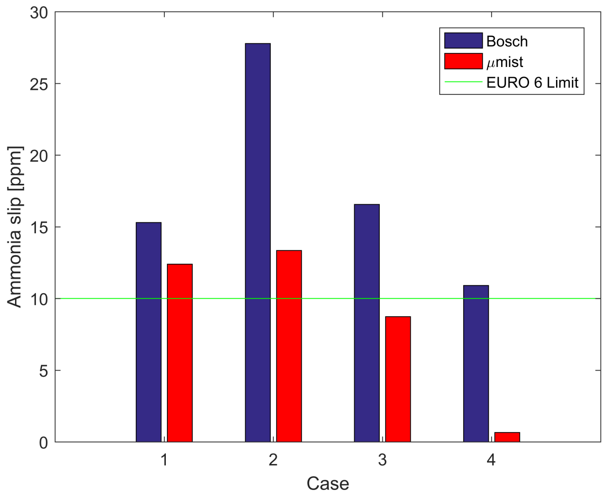

Figure 7.17: The overall ammonia slip for all the tested cases. The different color coding represent the two different dosers. The x-axis describes the different cases and the Y-axis the corresponding ammonia slip measured in [ppm].

There is less difference between the two different pipe settings but the mixer tends to have a larger impact on the measured ammonia slip results. The droplets have more time to evaporate prior the catalyst and conversion can be initiated earlier in the catalyst and overall less ammonia passes through when a mixing plate is installed. The limit of 10ppm can be achieved using the novel injector technology together with the standard mixing plate without using ammonia slip catalyst for these particular engine conditions.

7.4 Summary

An overall conclusion for both studies is that small preheated droplets injected with a highly dispersed cone have a great impact on overall NOx conversion and ammonia slip reduction. A mixer plate enhances the evaporative process resulting in higher conversion rates and lower ammonia slip. The exhaust flow structure prior the catalyst has an impact on the NOx conversion results and the activation temperature of the catalyst has been reduced compared to today's standard technologies.

Chapter 8

Heavy-Duty Testing

This chapter summarises the heavy-duty activities. The aim for this study is to investigate the performance of the novel injector technology with a market leading system. The investigation was conducted with and without a mixer plate in order to show the difference in conversion efficiency and ammonia slip.

8.1 Rig Setup

The main difference with this study compared to the initial light-duty testing is mainly the test engine and consequently higher exhaust mass flows. The test engine for this study was a full-size Scania D13 engine. To be able to fit this engine into the test facilities at Lund University minor modifications have been made. The standard turbo-charger has been replaced in order to have some more degrees of freedom in terms of inlet pressure. The intake air temperature can also be controlled with a fitted thermal management system. The complete setup can be seen in Figure 8.1 and the geometry is described in Table 8.1.

Table 8.1: The Scania D13 engine geometry

Displaced Volume [cc]	12740
Stroke [mm]	160
Bore [mm]	130
Compression Ratio [-]	18:1
Number of Cylinders [-]	6

A water-cooled pressure sensor is installed in every cylinder to have a complete sample of the in-cylinder pressures at a resolution of 0.2 CAD. The inlet air flow

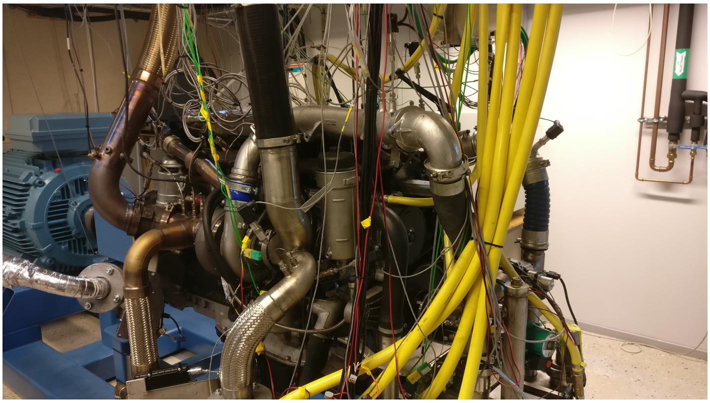

Figure 8.1: The engine setup that was used during this investigation. The figure describes the Scania D13 engine.

is measured with a hot film air mass flow sensor. The exhaust flow is calculated through a sum of inlet air flow and fuel flow measured via a Coriolis effect mass flow meter. The assumption is that there is no air and fuel leakage between the inlet- and exhaust manifolds.

The SCR-setup is the Vanadium catalyst described in Table 7.2 and the inlet flow pipe configuration from Figure 7.4. The mixer plate used in this study is also the same as for the previous setup.

8.2 Methodology

The measurement procedure during this study was kept constant during all the tested conditions. The SCR-catalyst was re-generated before any measurement and the target value for the regeneration was that the ammonia slip went to zero after the catalyst. The dosing was initiated when the engine was considered stable in terms of load and speed. The data acquisition was triggered when ammonia slip increased above 10ppm and the data was collected and averaged for the 100 consecutive cycles. The operating conditions presented in Table 8.2 was chosen from the full ESC test cycle [11].

8.3 Results

The catalyst temperature for all the tested conditions is shown in Figure 8.2.

For all the tested cases the exhaust temperature was kept stable and a target

Table 8.2: Summary of the test conditions for the heavy-duty operation

	Case 1		Case 2		Case 3		Case 4	
Speed [rpm]	1200		1400		1200		1400	
Description	With Mixer		With Mixer		No Mixer		No Mixer	
Load [bar]	4.5	8.75	4.5	8.75	4.5	8.75	4.5	8.75
Exhaust flow [kg/h]	225	310	310	375	225	310	310	375
AUS-32 Flow [kg/h]	0.5	0.85	0.4	1	0.5	0.85	0.4	1

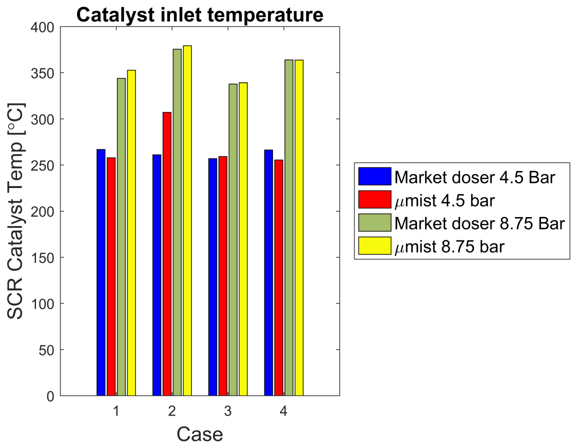

Figure 8.2: The inlet catalyst temperatures for all the tested cases. The x-axis describe the different tested setups and the y-axis the inlet temperature measured in [°C]

during the study was to achieve high enough SCR catalyst temperature to enable conversion with the cold AUS-32 injected by the market standard doser. The power output during the study can be seen in Figure 8.3.

The power output from the engine was also kept constant between all the tested cases. The dosing strategy during the study was calibrated with the novel injector and the flow rates were then transferred and kept constant for the market leading doser. The calibration target was highest possible conversion rate at the different speed and load cases.

Figure 8.4 shows the resulting NOx-conversion rates and with the mixer plate installed the conversion reaches almost 100% for all the tested conditions.

This result was expected due to high exhaust temperatures. With less flow restriction in terms of the removal of the mixer plate the difference is significant for the heavy-duty investigation. This is especially noticeable for the lower load cases where the small droplets generated by the novel injector has a great advantage.The NOx-conversion data can be converted to NOx emissions in terms of [g/kWh] and the results can be seen in Figure 8.5.

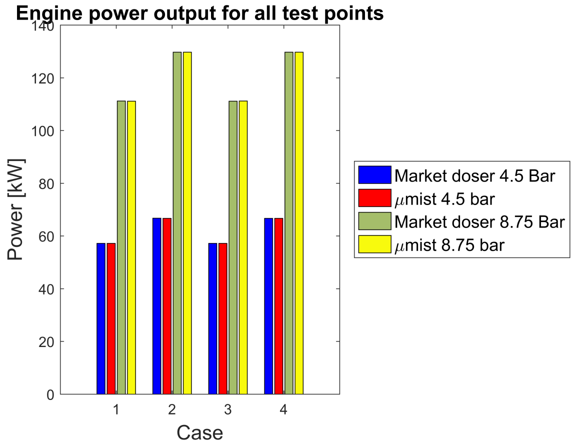

Figure 8.3: The measured engine power output for all the tested cases. The x-axis describes the different tested setups and the y-axis the engine power output measured in [kW].

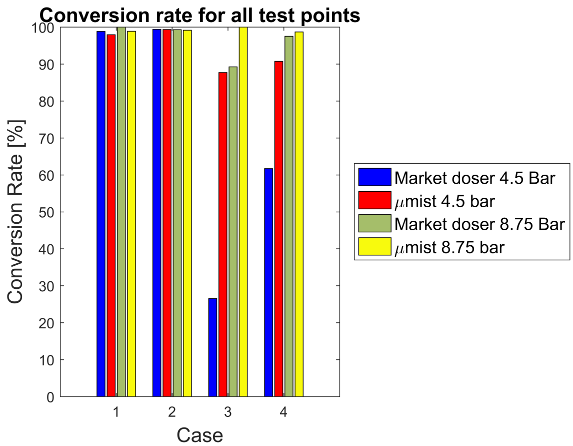

Figure 8.4: The measured conversion rate after the SCR Catalyst which represents how much NOx has been converted with in the catalyst for all the test points. The x-axis describes the different tested setups and the y-axis the conversion efficiency in [%].

All tested conditions resulting in a EURO VI pass except for the low load cases without the mixer plate installed. The ammonia slip however shows more diversity between the two tested injector technologies.

Figure 8.6 describes the ammonia slip results measured in [ppm] after the SCR-catalyst.The novel biomimetic injector achieves lower values than the regulated 10ppm [10] for all the tested cases and also significantly lower values than the market leading injector.

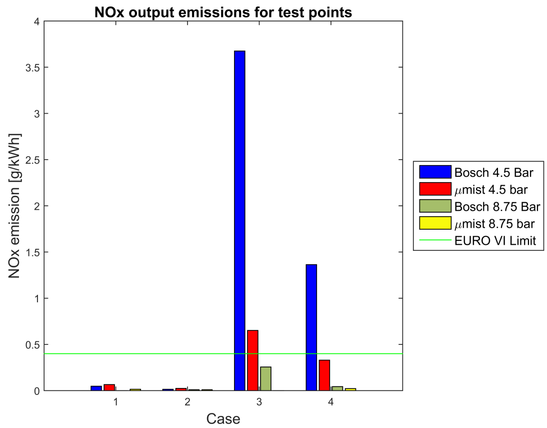

Figure 8.5: The NOx output emissions measured in g/kWh for all the test points. The green line represent the EURO VI limit of 0.4 g/kWh for heavy-duty engines. The x-axis describes the different tested setups and the y-axis the emissions in [g/kWh].

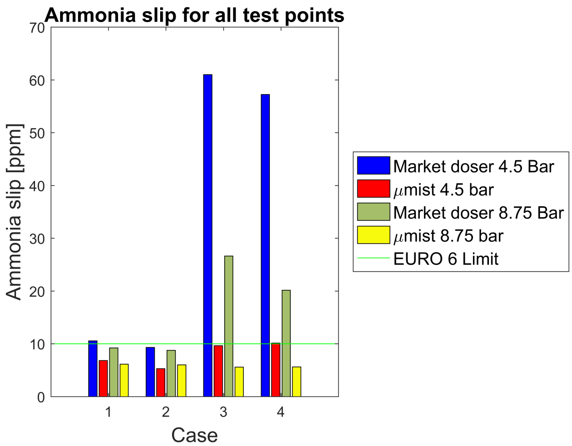

Figure 8.6: The ammonia slip for all the test points measured downstream of the SCR Catalyst. The x-axis describes the different tested setups and the y-axis the ammonia slip in [ppm].

8.4 Summary

This investigation shows the difference between the market leading doser technology and the novel biomimetic injector. The preheated well dispersed fine spray plume has shown a great potential for heavy-duty vehicle exhaust systems. A significantly better NOx-conversion results has been shown without a mixer plate installed resulting in a EURO VI pass considering both NOx emissions and ammonia slip. With less flow restriction between the engine and the

SCR-catalyst an improvement in CO_2 emissions can be achieved.

Chapter 9

Conclusions

This section concludes the results presented in this thesis. The main conclusion from the investigations is that the small preheated droplets generated by the μMist injector that mix well with the exhaust gases and evaporate faster than the market leading solutions. This provides a potential for future reduction of NOx emissions from diesel engines. The more specific conclusions are:

- Droplet sizes at $< 10\mu$m have been shown when the chamber temperature reaches 190°C.
- The novel biomimetic effervescent injector reduces the droplet sizes by 33% in SMD compared to the other more novel technologies and up to a 87% compared to the market leading solution.
- Above 98% NOx-conversion was measured during the investigation and for most conditions the ammonia slip was kept below 10 ppm with the novel injector.
- Good capability in reducing the light-off temperature whilst showing up to 98% conversion at average catalyst temperature of 200°C .
- High conversion, low ammonia slip and good mixing when using a flow restricted mixer plate but also capability to reduce the slip without one compared to the market systems.
- μMist injector technology has the potential to meet the future emission regulations for heavy-duty engines whilst reducing exhaust back pressure and therefore reducing fuel consumption and CO_2 emissions.

Chapter 10

Future Work

This section describes some of the planned and proposed future work regarding the biomimetic effervescent injector unit. Since this doser is very novel in its design phase and research area there is much to be considered before the product can be introduced to the market.

- The dosing unit needs to be investigated further in terms of controllability. Both matching the current target mass flow and also be able to vary the mass flow with a controller. This is the first step towards integrating the unit with a vehicle ECU for transient capability.
- More fundamental research is needed to fully understand the processes within the constant volume chamber. Observations during this work indicates that the internal pressure interacts with timings and this can be optimised for changes in droplet size and cone shapes.
- More design work and heat transfer optimisation is needed for the doser to be viable in terms of energy usage during continuous operation. The choice of main heat source is also a field that could be investigated to a further extent.
- Full exhaust emission certification cycle operation to investigate the complete performance specification and comparison when the dosing unit is more optimised and prepared for transient drive cycles.
- Research in other spray related areas to be able to use this technique in other applications and working fluids.

Chapter 11

References

[1] A. Anand. Selective catalytic reduction (scr) market research report- forecast to 2023, 2019.

[2] S. Anenberg, J. Miller, R. Minjares, L. Du, D. Henze, F. Lacey, C. Malley, L. Emberson, V. Franco, Z. Klimont, and C. Heyes. Impacts and mitigation of excess diesel related nox emissions in 11 major vehicle markets. *Nature*, 545:467–471, 2017.

[3] N. Beheshti and A. Mcintosh. The bombardier beetle and its use of a pressure relief valve system to deliver a periodic pulsed spray. *Bioinspiration and Biomimetics*, 2:57–64, 2007.

[4] N. Beheshti, R. Walker, L.-U. Larsson, A. Copestake, and A. McIntosh. "μmist® - the next generation fuel injection system: Improved atomisation and combustion for port-fuel-injected engines". SAE International, 08 2011. doi:10.4271/2018-01-1761.

[5] Y. Cengel and M. Boles. *"Thermodynamics - An Engineering Approach"*. "Sixth Edition". "McGraw-Hill Book Co, New York, US", 2007.

[6] M. Chen and S. Williams. Modelling and optimization of scr-exhaust aftertreatment systems. In *SAE Technical Paper*. SAE International, 04 2005. doi:10.4271/2005-01-0969.

[7] Cummins. Cummins filtration “adblue® q and a - aqueous urea solution (aus 32) for nox reduction in diesel engines.

[8] L. Cummins. *"Internal Fire"*. "Third Revised Edition". "Carnot Press, Oregon, US", 2000.

[9] J. Dec. A conceptual model of di diesel combustion based on laser-sheet imaging. In *SAE Technical Paper*. SAE International, 02 1997. doi:10.4271/970873.

[10] Dieselnet. Euro 6 emission legislation for heavy-duty trucks, 2018.

[11] Dieselnet. European stationary cycle, 2018.

[12] J. Dulae. Global transport outlook to 2050, 2012.

[13] Emitec. Heated catalysts, the solution to future emission problems, 2011.

[14] C. Fenimore. Formation of nitric oxide in premixed hydrocarbon flames. In *Symposium (International) on Combustion*, volume 13, pages 373–380. Elsevier, 1971. doi:10.1016/S0082-0784(71)80040-1.

[15] J. Girard, G. Cavataio, and C. Lambert. The influence of ammonia slip catalysts on ammonia, n2o and nox emissions for diesel engines. In *SAE Technical Paper*. SAE International, 04 2007. doi:10.4271/2007-01-1572.

[16] A. Haagen-Smit. Chemistry and physiology of los angeles smog. *Industrial and Engineering Chemistry*, 44(6):1342–1346, 06 1952. doi:10.1021/ie50510a045.

[17] M. Habib, M. Elshafei, and M. Dajani. Influence of combustion parameters on nox production in an industrial boiler. *Computers and Fluids*, 37(1):12–23, 01 2008. doi:10.1016/j.compfluid.2007.04.006.

[18] J. Heywood. *"Internal Combustion Engine Fundamentals"*. "Automotive Technology Series". "McGraw-Hill Book Co, New York, US", 1988.

[19] J. Houghton, Y. Ding, D. Griggs, M. Noguer, P. van der Linden, X. Dai, K. Maskell, and C. Johnson. Climate change 2001: The scientific basis. In *Intergovernmental Panel on Climate Change*. Cambridge University Press, 2001.

[20] IEA. International energy outlook 2018, 2018.

[21] M. Iwasaki and H. Shinjoh. A comparative study of "standard", "fast" and "no2" scr reactions over fe/zeolite catalyst. *Applied Catalysis A: General*, 390(1):71 – 77, 2010. doi:10.1016/j.apcata.2010.09.034.

[22] T. Johannessen, T. Schmidt, H. Svagin, J. Johansen, J. Oechsle, and R. Bradley. Ammonia storage and delivery systems for automotive nox aftertreatment. In *SAE Technical Paper*. SAE International, 04 2007. doi:10.4271/2008-01-1027.

[23] C. Johansson, L. Burman, A. Hanberg, U. Stenius, and M. Berglund. Swedish mk1 diesel versus european en 590 diesel – comparing the impact on emissions and health risks in the metropolitan area of stockholm. Report, ENVIRONMENT AND HEALTH ADMINISTRATION, 2012.

[24] S. Kim, T. Kuboyama, and H. Suzuki. "0d modeling of real-driving nox emissions for a diesel passenger vehicle". In *SAE Technical Paper*. SAE International, 09 2018. doi:10.4271/2018-01-1761.

[25] P. Kowalczuk and J. Drzymala. Physical meaning of the sauter mean diameter of spherical particulate matter. In *Particulate Science and Technology*, volume 34, pages 645–647. Taylor and Francis, 2016. doi:10.1080/02726351.2015.1099582.

[26] G. Lavoie, J. Heywood, and J. Keck. Experimental and theoretical study of nitric oxide formation in internal combustion engines. *Combustion Science and Technology*, 1(4):313–326, 1970. doi:10.1080/00102206908952211.

[27] N. Leahey, R. Crawford, J. Douglas, and J. Bauman. Induction heating of catalytic converter systems and its effect on diesel exhaust emissions during cold start. In *SAE Technical Paper*. SAE International, 04 2018. doi:10.4271/2018-01-0327.

[28] P. Malte and D. Pratt. Measurement of atomic oxygen and nitrogen oxides in jet-stirred combustion. *Fifteenth Symposium (International) on Combustion*, 15(1):1061–1070, 1975.

[29] A. McIntosh and J. Lawrence. The extraordinary design of the bombardier beetle — a classic example of biomimetics. In *Eighth International Conference on Creationism*, pages 268–276. ICC, 2018.

[30] A. Mellor, J. Mello, K. Duffy, W. Easley, and J. Faulkner. Skeletal mechanism for nox chemistry in diesel engines. In *SAE Technical Paper*. SAE International, 04 1998. doi:10.4271/981450.

[31] I. Nova and E. Tronconi. *Urea-SCR Technology for deNOx After Treatment of Diesel Exhausts*. "Fundamental and Applied Catalysis". "Springer", 2014.

[32] OKQ8. Okq8 diesel - miljöklass 1, 2011.

[33] S. Schmieg and J. Lee. Evaluation of supplier catalyst formulations for the selective catalytic reduction of nox with ammonia. In *SAE Technical Paper*. SAE International, 10 2005. doi:10.4271/2005-01-3881.

[34] G. Stumpp and W. Banzhaf. An exhaust gas recirculation system for diesel engines. In *SAE Technical Paper*. SAE International, 02 1978. doi:10.4271/780222.

[35] R. Suarez-Bertoa, P. Mendoza-Villafuerte, P. Bonnel, V. Lilova, L. Hill, A. Perujo, and C. Astorga. On-road measurement of nh3 and n2o emissions from a euro v heavy-duty vehicle. *Atmospheric Environment*, 139:167 – 175, 2016. doi:10.1016/j.atmosenv.2016.04.035.

[36] H. Wang, R. Xu, Y. Jin, and R. Zhang. Zeolite structure effects on cu active center, scr performance and stability of cu-zeolite catalysts. *Catalysis Today*, 2018. doi:10.1016/j.cattod.2018.04.035.

[37] J. Yang, V. I. Golovitchev, P. R. Lurbe, and J. J. L. Sánchez. Chemical kinetic study of nitrogen oxides formation trends in biodiesel combustion. In *International Journal of Chemical Engineering Volume 2012*, volume 2012, page 22 pages. Hindawi, 2012. doi:10.1016/S0082-0784(71)80040-1.

[38] L. Yuejin, R. Stan, D. Joe, and B. Tilman. Effects of lean/rich timing and nature of reductant on the performance of a nox trap catalyst. *Topics in Catalysis*, 16(1):139–144, Sep 2001. doi:10.1023/A:1016651418882.

[39] J. Zeldovich. The oxidation of nitrogen in combustion and explosions. In *HERO*, volume 21, pages 577–628. Health Environmental Research Online (HERO), 1946.

Scientific publications

Author contributions

Paper I: A Droplet Size Investigation and Comparison Using a Novel Biomimetic Flash-Boiling Injector for AdBlue Injections

This paper present a droplet size investigation and a comparison with this new method of injecting AUS-32 into the stream of exhaust gases. I did the experiments, design of the experiment and the analyse of the data and I wrote the paper. Will Lennard had the lead in designing the new novel injector technology and the other authors contributed to the paper with discussions and proof reading the final paper before submission. I presented the paper in Baltimore, US 2016.

Paper II: NOx-Conversion and Activation Temperature of a SCR-Catalyst Whilst Using a Novel Biomimetic Flash-Boiling AdBlue Injector on a LD Engine

This paper present a NOx-Conversion and Activation temperature investigation conducted on a Light-Duty engine. I had the lead in designing the experiment and building the experimental setup. I did the experiment and run the dosing unit during the experiments. I analyse the results and wrote the paper. Will Lennard had the lead in designing the parts and Jessica Dahlstrom run the test engine during the tests. The other authors contributed with discussions and proof reading before submission. I present the paper in Baltimore, US 2016.

Paper III: SCR-Catalyst Utilisation and Mixing Comparison using A Novel Biomimetic Flash-Boiling Injector

This paper present a SCR-Catalyst utilisation and mixing comparison between the novel injector and a market leading technology. I had the lead in designing the experiment and building the experimental setup. I did the experiments and analysed the results. I wrote the paper. The other authors contributed with discussions and proof reading before submission. I present the paper in San Diego, US 2018.

Paper IV: NOx-Conversion Comparison of a SCR-Catalyst Using a Novel Biomimetic Effervescent Injector on a Heavy-Duty Engine

This paper present a Nox-Conversion study and comparison between the novel injector with a market leading standard system performed on a Heavy-Duty engine setup. I had the lead in designing the experiment and building the experimental setup. I did the experiments, analysed the results and I wrote the paper. The other authors contributed with discussions and proof reading before submission. I present the paper in San Antonio, US 2019.